Design, synthesis, and studies on thermodynamic and biological activities of lanthanide (III) complexes of hydrazinecarbothioamide ligands

U. B. Amadi*, M. Ogwuegbu, C. K. Enenebeaku, G. Onyedika, C. O. Akalaezi, C. O. Alisa

Department of Chemistry, Federal University of Technology, Owerri, Imo State, Nigeria

Abstract

New tetradentate ligands, 2-(2-hydroxybenzoyl)hydrazinecarbothioamide, HL1, and 2-(2-mercaptobenzoyl)hydrazinecarbothioamide, HL2, were designed and synthesized from the condensation reactions of salicylic and, thiosalicylic acids with thiosemicarbazide in one pot without any coupling agent. The ligands were characterized using physical and spectroscopic methods. They formed complexes with Nd (III) and Dy (III) ions. The FTIR results suggest that the ligands exhibit azo-hydrazo tautomerism. The complexes were thermally stable with NdHL1 having a decomposition activation energy, Ea of 54.7 kJmo^{-1}, ΔH value of 47.8 kJmol^{-1}, ΔS value of -23.1 kJmol^{-1}, ΔG value of 237.8 kJmo^{-1} being the most stable at 530 C. The dysprosium complexes were crystalline, while the neodymium complexes were amorphous and produced no peaks in X-ray diffraction spectra. The complexes have the general formula [Ln (HL)$_2$(H$_2$O) $_m$(NO$_3$) $_n$] (H$_2$O) $_m$(NO$_3$) $_n$, where m ranged between 0 and 2, while n ranged from 0 to 1. The complexes showed thermal stability beyond 400 ∘C. All the compounds showed significant antimicrobial activities against aspergillus flavus at concentrations of 12.5, 25, and, 50 mg/ml, with the highest activity recorded at 50 mg/ml for DyHL2. DyHL2 complex also showed the highest binding affinity of 5.3 kcal/mol, compared to the binding affinities -1.3, kcal/mol, -1.2, -5.2, 5.1, and -5.0 kcal/mol obtained for HL1, HL2, NdHL1, NdHL1, DyHL1 and NdHL2 respectively from molecular docking studies, indicating inhibitory efficacy against A. *f*lavus. The complexes are potential novel compounds for the development of drugs, photocatalysts, photosensitized materials, and photocells used in organic synthesis, and solar energy conversion devices.

Communicated by: D. K. Sahoo

1. Introduction

Amides are important functionalities in molecular science due to their presence in peptide and proteins. The synthesis of amides and their derivatives are of great importance due to their well ubiquitous presence in biological systems [1, 2]. They generally contain R-CO-NHR functional group [3]. Amide bonds, C-N are important integral part of too many pharmaceutical, polymer and natural products and proteins [1]. Generally, hydrazinecarbothioamide derivatives, HCTA, have been reported to be synthesized from Isothiocyanines and hydrazides or hydrazine. Hydrazinecarbothioamide are biologically active intermediates with various application in the synthesis of

*Corresponding author Tel. No: +234-803-326-1235.
Email address: buamadi@akanuibiampoly.edu.ng (U. B. Amadi)

other scaffolds in [4–10]. Hydrazincarbothioamides derivatives of thiosemicarbazide have numerous potentials as antimicrobial, antifungal anti-cancer and other applications including as anti-corrosion agents. These properties have made them target molecules in medical, industrial, electronic and pharmaceutical research [4, 11–13].

The past two decades, have experienced the emergence of several fascinating and exciting areas associated with the coordination chemistry of lanthanide elements, involving dealings with macrocyclic ligands, new extraction processes, self-assembled supra molecular edifices, hetero-metallic d-f compounds, coordination's in ionic ligands, lanthanoidomesogens, lanthanoid-fullerenes, nanoparticles, crystal-to-crystal reactions, coordination polymers (CPs) etc. [14]. Most of the compounds mentioned earlier are fluorescent. Lanthanide (III) ions luminescence property is highly desirable for sensing and imagine due to their characteristic emission wavelengths, long decay lifetime(half-life) and large pseudo strokes shifts of sensitized emissions. The long lifetimes enable time-gated detection of the emission, which results to spectra with large signal to noise ratios. The D-F transitions are parity – forbidden, which poses a challenge for direct excitation. Coordinated ligands are used to absorb light and transfer energy to the Lanthanide (III) ion to achieve Lanthanide (III) centered emission. The antenna effect of the ligand enables the metal center luminescence [15].

Researchers have over the years devoted attention to the search for suitable organic extractants for the extraction and processing of rare earth metals, especially lanthanides.

This is due to the selectivity of the elements towards the available organic extractants [16]. hydrazinecarbothioamides are known reactive intermediate. The presence of O, N,S atom carrying electron pairs make these ligands suitable extractants for the study of lanthanide coordination chemistry [15]. The importance of the lanthanides in various facets of human needs cannot be overemphasized. This is mainly due to the wide range of applications of the lanthanide complexes spanning the medical industries in diagnosis and treatment, as MRI agents, theragnostic and in the rapidly developing field of pharmaceutical inorganic chemistry [4]. In electronics as diodes, in solar cells and photosensitized materials, in sophisticated military equipment and mobile phones. The design and synthesis of new organic compounds for the study of dysprosium and neodymium complexes are desirable. Their unique properties have positioned their complexes as excellent fluorescent and contrast agents in spectroscopic probes, lasers and sensors. Their compounds have been reported to possess magnetic, optical and catalytic properties and also find applications as biosensors [17, 18]. Their luminescence and photophysical properties have recently found applications in imaging in visible region and in the near infrared region [19–21].

Although, the synthesis was challenging as the synthesis was not carried out with usual coupling agents such as N,N-dicyclohexylcarbodiimide (DCC), for the synthesis of amide [1]. The various applications of lanthanide complexes of organic compounds make it extremely important to study the thermal stability profile of new lanthanide complexes so as to explore their numerous applications in various industries [22, 23].
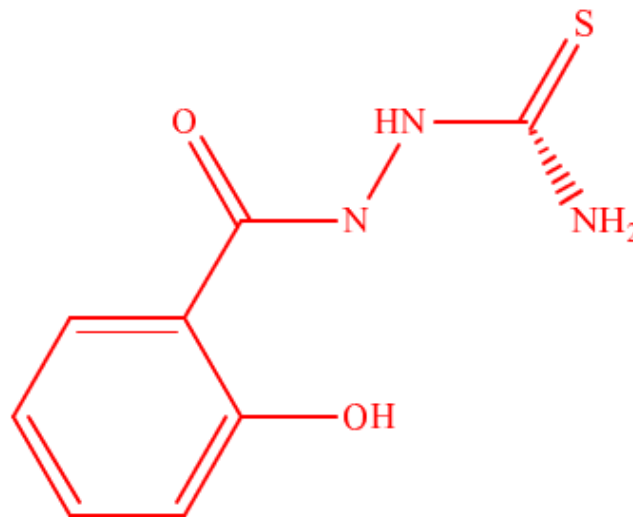

Figure 1. Structure of 2–(2–hydroxybenzoyl) hydrazinecarbothioamide ligand (HL1).

Thermogravimetric analysis, TGA used in the study has since been widely deployed in the investigation and evaluation of thermal stability of complexes and polymers, to ascertain their applications at high temperature processes [24, 25]. Lanthanide complexes, generally have been reported to show thermal stability up to 300 °C [26].

In this present work, we focused on the synthesis of new and novel low molecular weight hydrazinecarbothioamide compounds derived from thiosemicarbazide and carboxylic acids and their dysprosium, Dy and Neodymium, Nd complexes. The coupling of the carboxylic acids with thiosemicarbazide without a coupling agent was quite challenging and the process was nearly abandoned. It took the formation of needle-like crystals of the compounds on the flasks left unwashed to continue the synthesis. Coupling agents were not used in other to achieve a one pot synthesis, save cost, make the synthesis direct and less cumbersome. This could be the reason for the absence of precipitates as expected from literature. The molecular structures of the compounds were determined using various spectroscopic and chromatographic techniques. The complexes formed with the novel hydrazinecarbothioamide ligands were studied for their thermal stabilities using the modified Coat-Redfern's model. The compounds were subjected to invitro and in vivo studies.

2. Experimental reagents

All chemicals used were of analytical grade, 99.999 % purity. The reagents and solvents used in all the synthesis were purchased from Sigma Aldrich and Merch (Sigma-Aldrich). The reagents for the chemical synthesis and the instruments used for the characterization are presented in Table 1.

Table 1. Experimental reagents.

Reagents	Instruments
Thiosemicarbazide	UV-VIS Spectrophotometer
Thiosalicylic acid	UV-VIS Cary 3500
Salicylic acid	CE-440 Elemental Analyzer
Neodymium (III) nitrate hexahydrate	BRUKER 600 Hz,USA
Dysprosium (III) nitrate hexahydrate	
	Rigaku mini flex 600 Japan XRD
	Perkin 4000 thermal analyzer
Ethanol	Agilent 7890A Gas Chromatograph
	5977MSD Inert Mass Spectrometer
	Autoclave-E-track Scientific Instrument Italy

Table 2. Physical and analytical characterization of the lanthanide III complexes.

S/N	Compound	Color	Melting Pt(C)°	Yield	Molar Nature of Structure/ (%)	conductivity (Ω^{-1}cm2 mol-1)	complex geometry
1	[Nd($C_8H_9N_3O_2S$)$_2$(H_2O)]NO_3	Deep Purple	280-282	65	139	Electrolyte	Bicapped square antiprism
2	[Nd($C_8H_9N_3OS_2$)$_2$(H_2O)]NO_3	Grey	284-286	73	132	Electrolyte	Bicapped square antiprism
3	[Dy($C_8H_9N_3O_2S$)$_2$(NO_3)]	DarkMagenta	285-287	83	35	Non-electrolyte	TricappedTrigonalPrismatic
4	[Dy($C_8H_9N_3OS_2$)(H_2O)]NO_3	Dark Brown	297-300	85	147	Electrolyte	Bicapped square antiprism
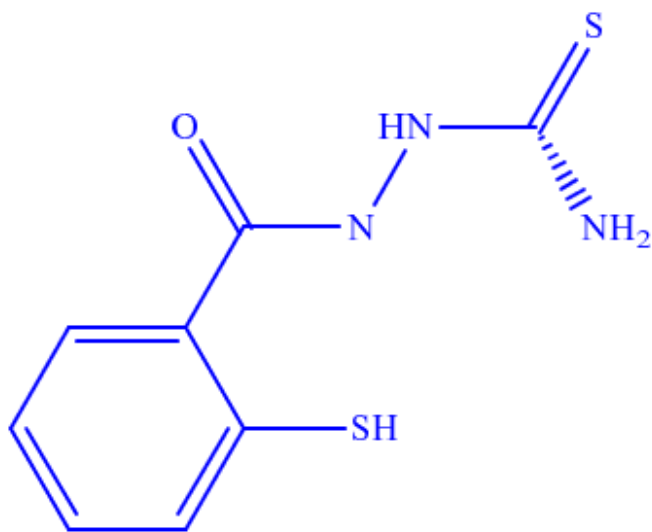
Figure 2. Structure of 2-(2-mercaptobenzoyl) hydrazinecarbathioamide ligand (HL2).

3. Synthesis of ligands

3.1. Preparation of (HL$_1$)

Step 1: A mixture of Salicylic acid (0.96 g, 0.1 mol) and thiosemicabazide (0.46 g, 0.1 g) in 50 ml of ethanol were refluxed for 4 hours at 80 C and pH of 7.6.

Step 2: The resulting solution was filtered cooled under ice, and the filtrate were evaporated to remove the solvent.

Step 3: The crystals formed were washed with cold ethanol and then recrystallized with ethanol to give brown needlelike crystal.

Step 4: After drying, the melting point and percentage yield were determined, modified [27].

Crystalline Yield: 78%, m.p 147-153 °C Analysis: FTIR (KBr, cm^{-1}):3429(O-H), 33362(N-H)3011-2922(C-H), 1654(C=O)1530(C=C).UV-Vis., (DMSO,nm):310,315(λ max), 335,345. ^{1}HNMR (600 MH$_Z$, CDCl$_3$) δ = 3.33–3.41ppm (NH2), 6.810 – 6.822ppm (ArHC-H), 7.36 – 7.38ppm (ArH(CH)), 7.87 – 7.90ppm (NH), and 4.62 - 5.0ppm(C=O).MS(EI,70 Ev): calcm/z(%) = 211[M +4]$^+$. Analysis for C$_8$H$_9$N$_3$O$_2$S (211.45): Calcd., 211.24,C,45.12; H,4.13; N,19.43; O,14.91; S,15.01. Found: C,45.49;H,4.29;N19.89;O15.15;S15.18.

3.2. Preparation of (HL$_2$)

Step 1: A mixture of thiosalicylic acid (0.77 g, 0.1 mol) and thiosemicarbazide (0.46 g, 0.1 g) in 50 ml of ethanol was refluxed for 4 hours at 80 C and pH of 7.6.

Step 2: The resulting solution was filtered, cooled under ice and the filtrate was evaporated to remove the solvent and the white needle- like crystals left behind were washed with cold ethanol and recrystallized with ethanol.

Step 3: After drying, the melting point and percentage yield were determined.

Crystalline Yield: 88%, m.p 153-157 °C. Analysis: FTIR(KBr, cm^{-1}): 3749(O-H),3235(NH)3004(C-H_1654(C=O)130(C=C). hyUV Visi(DMSO,nm):372, 398, 412(λ max), 410. ^{1}NMR(600MH$_Z$, CDCl$_3$) δ = 3.28-3.30(NH2), 6.815-6.822(ArHC-H), 7.44-7.48(ArH(CH)), 7.88-7.90(NH) and 4.62 - 5.0(C=O). M/S(EI,70): found m/z(%) = 227[M]$^+$. Analysis for C$_8$H$_9$N$_3$OS$_2$ (228.03):Calcd., C, 42.15; H3.48;N,18.22; O,6.54; S,28.04. Found: C,42.27; H,3.99; N,18.49; O,7.04; S,28.21.
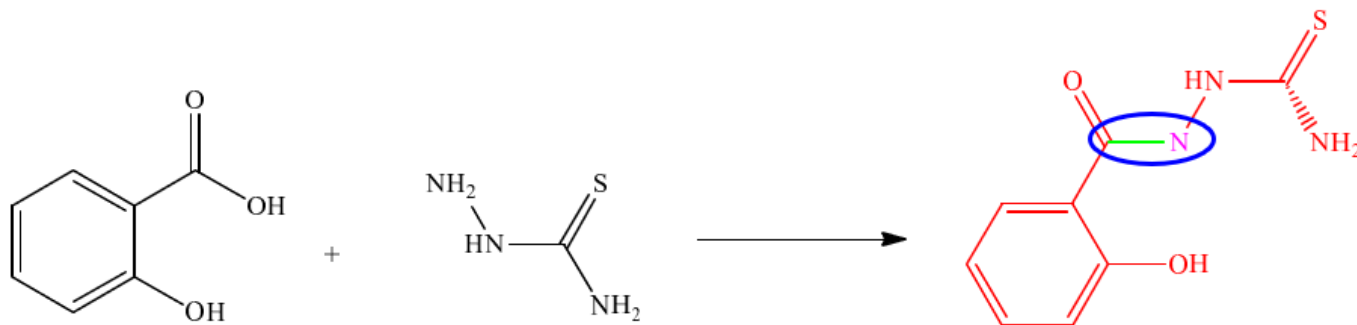
Figure 3. Synthesis of Fig 1: structure of 2–(2–hydroxybenzoyl) hydrazinecarbothioamide ligand (HL1).
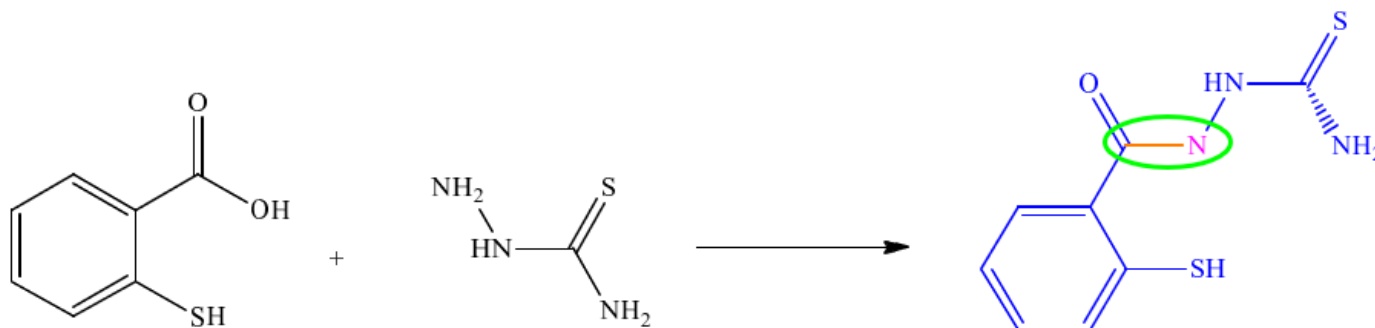

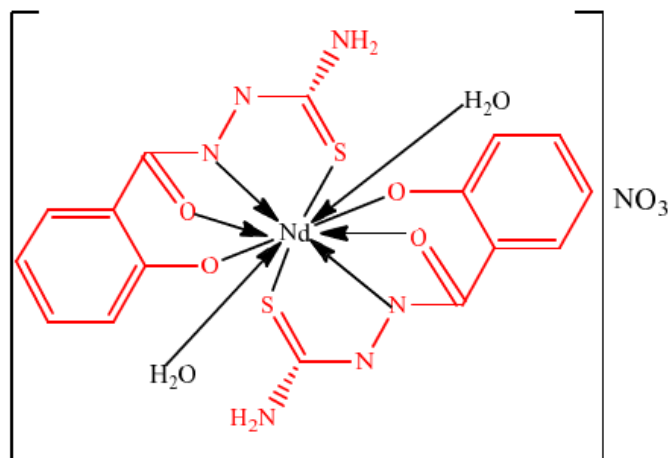Figure 4. Synthesis of 2-(2-mercaptobenzoyl) hydrazinecarbathioamide ligand (HL2).

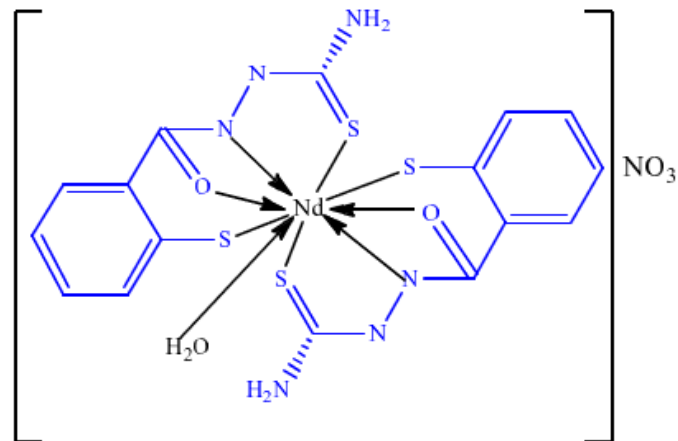Figure 5. Neodymium complex of 2–(2–hydroxybenzoyl) hydrazinecarbothioamide, NdHL1.

Figure 6. Neodymium complex of 2-(2-mercaptobenzoyl) hydrazinecarbathioamide, NdHL2.

4. Preparation of Lanthanide (III) Complexes: (Ln = La(III), Nd(III), Dy(III))

The lanthanide (III) complexes were prepared by refluxing the ligands I –II with the respective lanthanide nitrate salts in the metal-ligand ratio of 1:2. Exactly 20 ml of ethanolic solution of the ligand was refluxed with 10 ml of the various lanthanide nitrates dissolve in ethanol for 1 hour, and the solid product formed was separated and washed thoroughly with hot ethanol and then air dried.

4.1. Determination of molar conductivity

The molar conductivity measurement of the samples was carried out with a 10^{-3}M solution of the samples in DMSO, at 25 ± 0.5 ^{0}C. The conductivity was determined using a conductivity meter (HACH HQ40d).

4.2. Determination Of UV-Vis spectrum

The UV-Vis spectra of the prepared complexes (10^{-3} M), in absolute ethanol were recorded on a spectrophotometer (Carry3500 UV-Vis Spectrophotometer). The absorption of the

Table 3. UV-visible spectroscopic data for the ligands and their lanthanide complexes.

Compound	λ max (wave length, nm)	Wave number (cm^{-1})	Absorbance	ε_{max} Mole.cm^{-1}
HL1	310, (315), 335,345	31746	3.211	3211
HL2	372, 398, (412), 410	24272	0.200	200
NdHL1	(294), 208, 210, 221, 242	34014	10.00	10000
NdHL2	(295), 201, 212, 225, 237	33898	10.00	10000
DyHL1	303	33003	6.160	6160
DyHL2	(323)	30488	10.00	10000

Note: figures in bracket are the wavelengths of maximum absorption. The others are wavelengths where significant absorptions occurred.

Table 4. FTIR Spectroscopy Bands of the Ligands and Their Lanthanide Complexes in (Cm^{-1}).

Compound	v(O-H) Cd	v(C=O) cm^{-1}	v(C-N)	v(N-H)	v(N-N)	v(C=S)	v(Ln-N)	v(Ln-S)	v(Ln-O)	v(O-H) Ucd	v($^-$NO3)
HL$_1$	-	1654	1151	3362	1088	1382	-	-	-	3429	-
HL$_2$	-	1654	1150	3235	1089	1382	-	-	-	3749	-
NdHL$_1$	640	1541	1147	3348	1031	1335	405	453	526	-	820
NdHL$_2$	640	1513	1143	3085	1030	1334	402	459	504	-	811
DyHL$_1$	-	1594	1147	3230	1030	1296	425	455	511	-	813
DyHL$_2$	657	1594	1150	3232	1030	1323	431	460	530	-	813

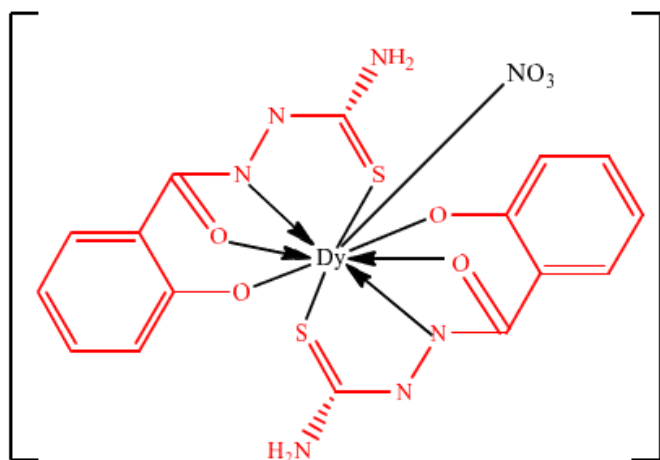**Key**: Ucd stands for uncoordinated water, Cd stands for coordinated water.

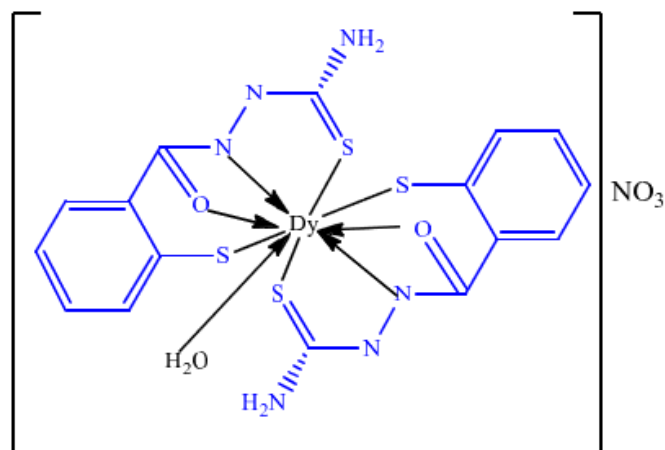Figure 7. Dysprosium complex of 2–(2–hydroxybenzoyl) hydrazinecarbothioamide, DyHL1.

Figure 8. Dysprosium complex of 2-(2-mercaptobenzoyl) hydrazinecarbathioamide, DyHL2.

solutions of all the complex in ethanol was scanned in the region between 200-800 nm, at a spectral band width of 2 nm. The absorbance versus wavelength spectral data were collected.

4.3. Determination Of FTIR spectroscopy

The FT-IR Spectra of the samples were obtained in the 4000-400 cm^{-1} range using Thermo-Fisher Scientific Carry 630FT-IR Spectrometer, equipped with KBr optics and complimentary diamond ATR accessories. The acquired interferogram was converted into a spectrum by Fourier Transformation.

4.4. Determination of elemental contents

The C, H, N, O and S Contents of the samples were determined by dynamic flash combustion, using an elemental analyzer (CE-440 Elemental Analyzer, Exeter Analytical Inc, UK). Sample weight used for the determination ranged from 1.0-1.5mg. The combustion and reduction temperature were
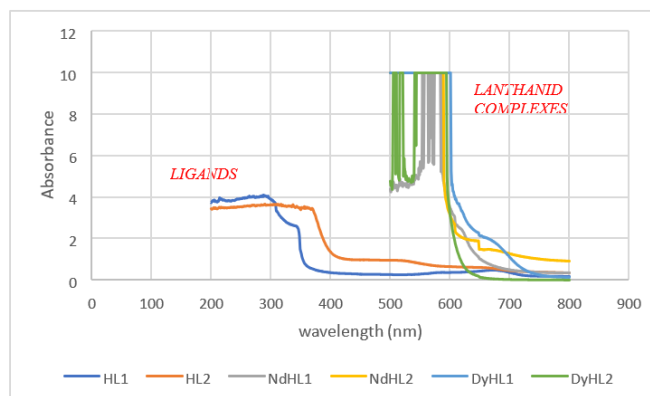

Figure 9. UV Visible spectral of the ligands vs complexes showing shift to a higher wavelength in the complexes due to complexation.
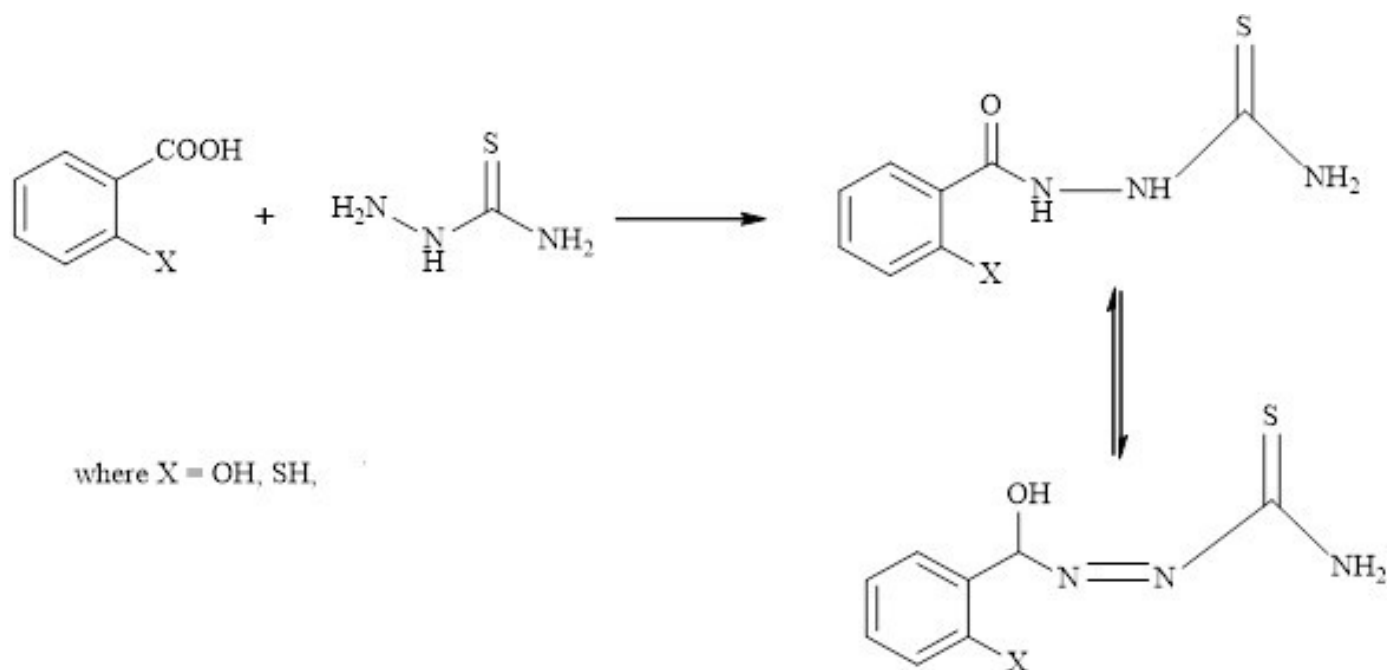
Figure 10. Tautomerism in the ligands.
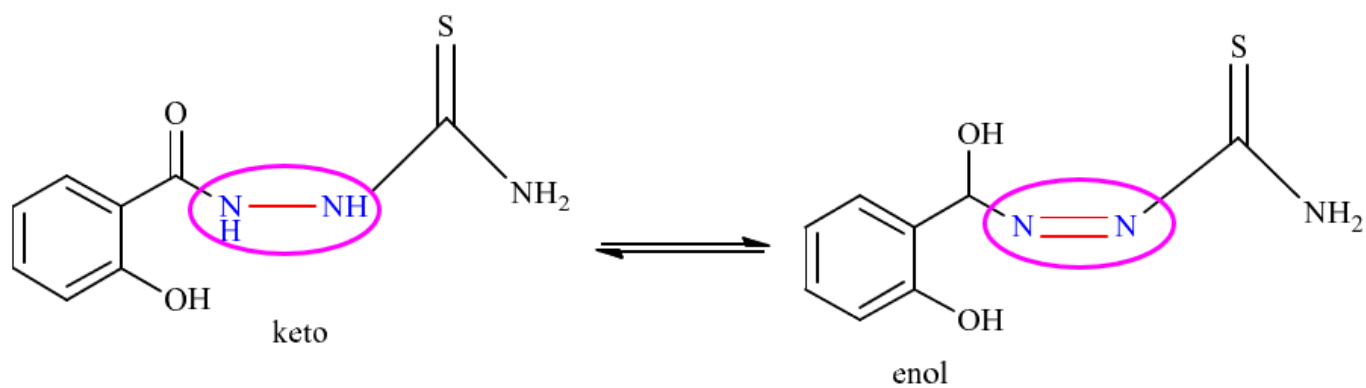
Figure 11. Tautomerism in 2–(2–hydroxybenzoyl) hydrazinecarbothioamide HL1 ligand.
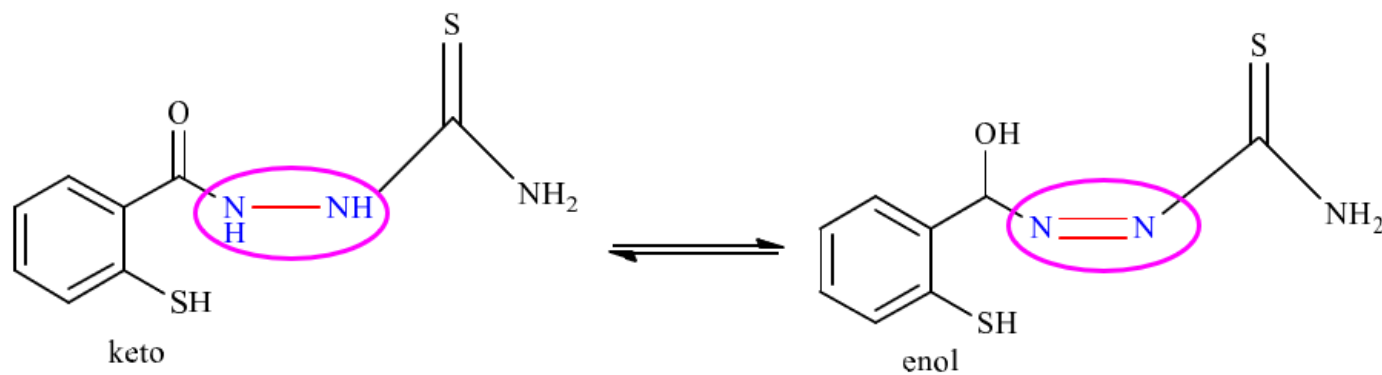
Figure 12. Tautomerism in 2-(2-mercaptobenzoyl) hydrazinecarbathioamide HL_2 ligand.

Figure 13. FTIR Spectral of in 2–(2–hydroxybenzoyl) hydrazinecarbothioamide HL1.
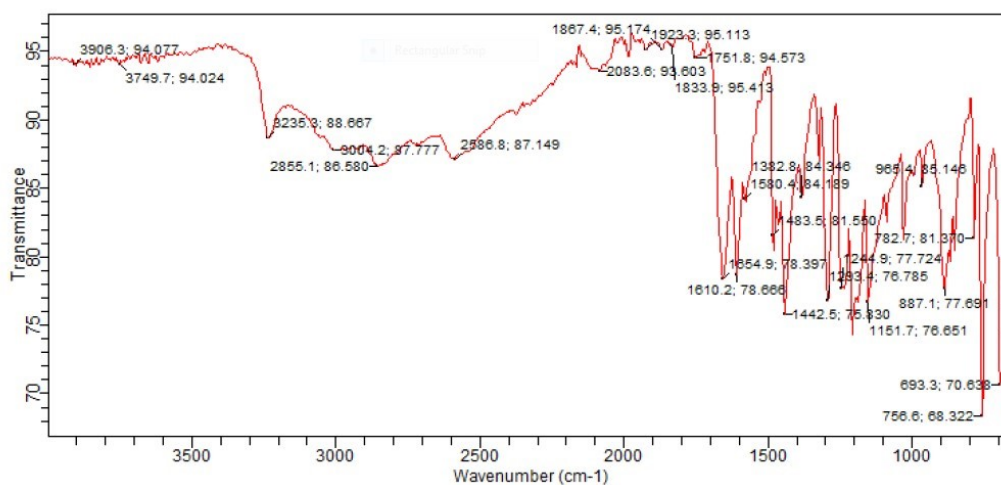
Figure 14. FTIR Spectral of 2-(2-mercaptobenzoyl) hydrazinecarbathioamide HL2.
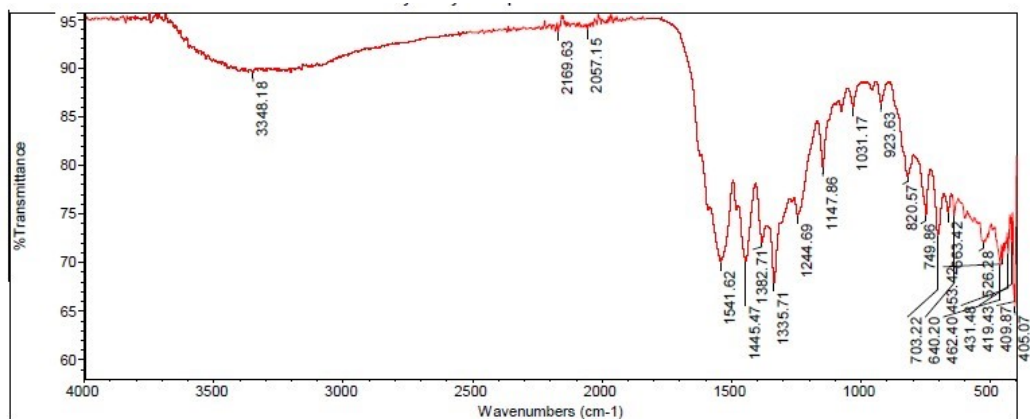
Figure 15. FTIR Spectra of Nd complex of 2-(2-hydroxybenzoyl)hydrazinecarbothioamide,NdHL$_1$ showing spectra shifts from the ligand due to complexation.

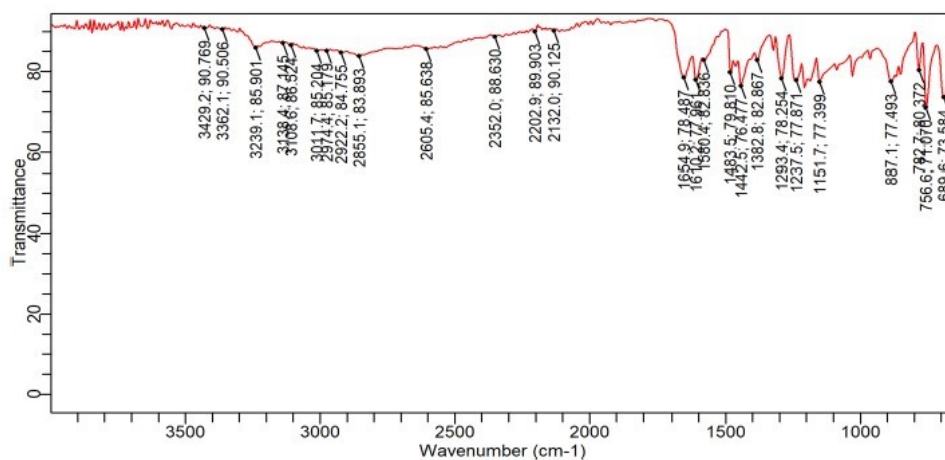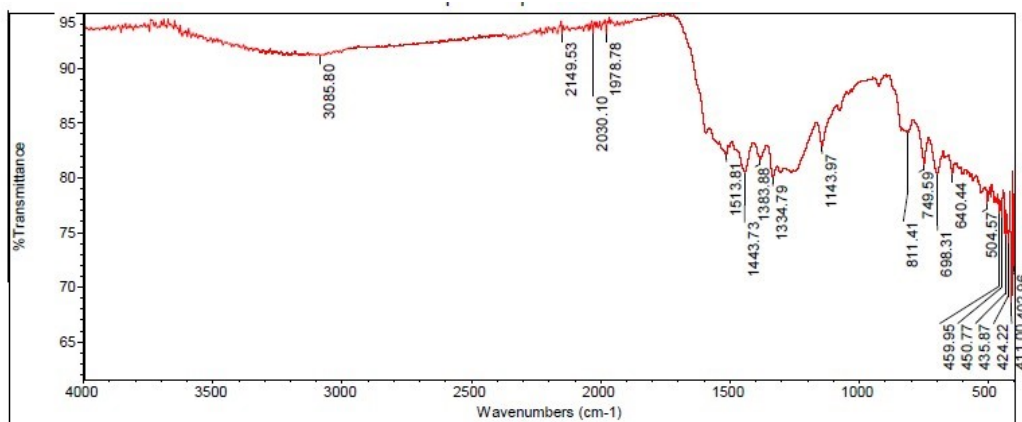Figure 16. FTIR Spectra of Nd complex of 2-(2-marcaptobenzoyl) hydrazinecarbothioamide,NdHL$_2$ showing spectra shifts from the ligand due to complexation.
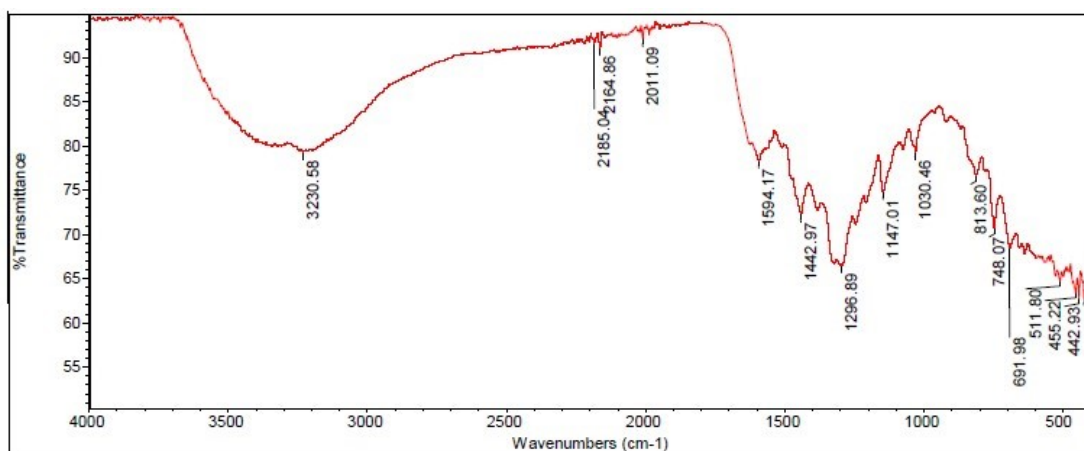
Figure 17. FTIR Spectra of Dy complex of 2-(2-hydroxybenzoyl)hydrazinecarbothioamide,DyHL$_1$ showing spectra shifts from the ligand due to complexation.
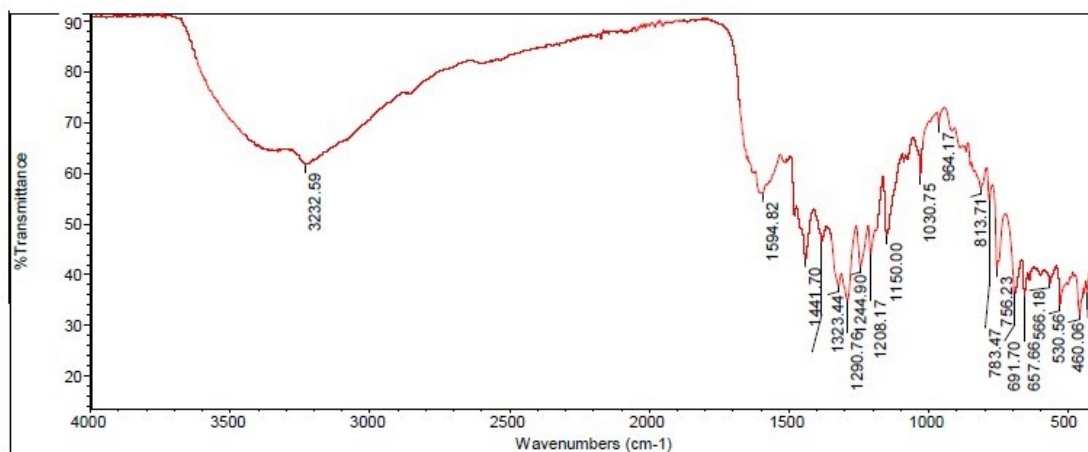
Figure 18. FTIR Spectra of Dy complex of 2-(2-marcaptobenzoyl) hydrazinecarbothioamide,DyHL$_2$ showing spectra shifts from the ligand due to complexation.

975 and 600°CC respectively while the oven temperature was 81°CC. The chromatographic column was Parapak PQS column, while the detector was thermal conductivity detector. The combustion products (N$_2$, CO$_2$) were detected and the content of each element was calculated from the second stage after pyrolysis and subsequent formation of carbon monoxide (CO).

Figure 19. HNMR spectra of 2-(2-hydroxybenzoyl)hydrazinecarbothioamide showing chemical shifts.

4.5. Determination Of G.C-Mass spectrometry of samples

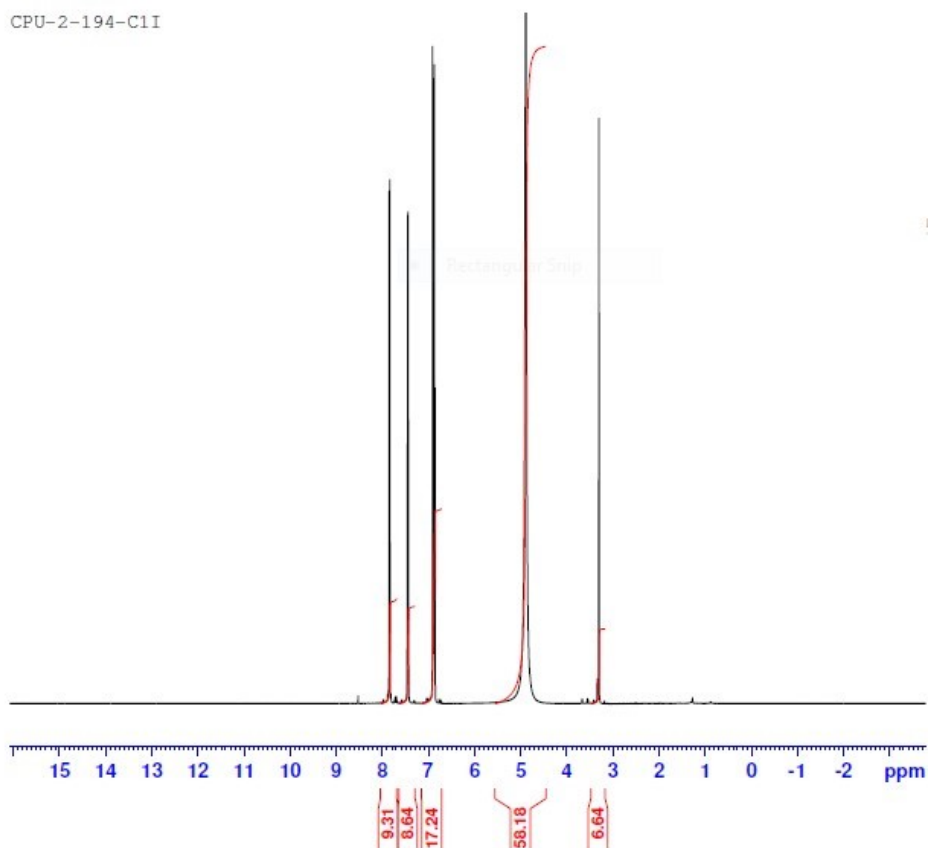The samples were analyzed using Agilent technologies 7890A GC and 5977B MSD with experimental conditions of GC-MS system as follows: Hp 5-MS capillary standard non-polar column, dimension 30M, ID: 0.25mm, Film thickness 0.25μm. Flow rate of mobile phase (carrier gas: He) was set at 1.0 ml/min. in the gas chromatography part. Temperature program (oven temperature) was 40°C raised to 250°C at 5°C/min and injection volume was 1 μl. Samples dissolved in methanol were run for fully scan at the range of 40-650 m/z and the results were compared by using Nist Mass Spectral Library Search Program.

4.6. Thermal analysis

TGA and DTA of the lanthanide complexes were carried out using Perkin 4000 Thermal Analizer.

The higher decomposition activation energy, Ea and the higher stability observed for NDHL1 can be attributed to the bicapped square antiprism, BSA geometry which is more symmetrical wit spatial compact which can lead to enhanced structural rigidity and increased stability compared to the other complexes. Other factors such as the ligand densely environment and electronic configuration can enhance the stability of NdHL1. The higher stability of DyHL1 compared to NdHL2 and DyHL2 can be attributed to the smaller ionic radius of Dy^{3+} which favors lower coordination numbers and enhance the stability of the TTP complex, thereby making it more stable than the BSA complexes of NdHL2 and DyHL2. The stability of NdHL1 complex can further be enhanced by the O and N donor atoms to the benzene ring of HL1 ligand. O and N are hard donor atoms and bind much more strongly to Nd^{3+} and Dy^{3+} which will result to increased thermally and chemical stability observed for NdHL1 and DyHL1 complexes compared to NdHL2 and DyHL2 containing S- donor atom attached to the benzene ring of HL2 which is a soft donor atom. The larger ionic radius of Nd^{3+} favors oxygen-based donors compared to the smaller ionic radius of Dy^{3+} which explains the higher activation energy obtained for NdHL1, making it most stable of the complexes and followed by DyHL1. This clearly demonstrates the effect of ligands on the stability of coordination complexes of these lanthanide ions. This finding agrees with the findings reported by Falco *et al.* [28]. Generally, the stability of lanthanide complexes is greatly influenced by the ligand selection, geometry and ionic radius. Reported the influence of ionic radius of Nd^{3+} and Dy^{3+} complexes of a semirigid ligand favored Dy^{3+} complex due to the smaller ionic radius of Dy^{3+}ion in a capped octahedral complex formed with the ligand [29, 30].
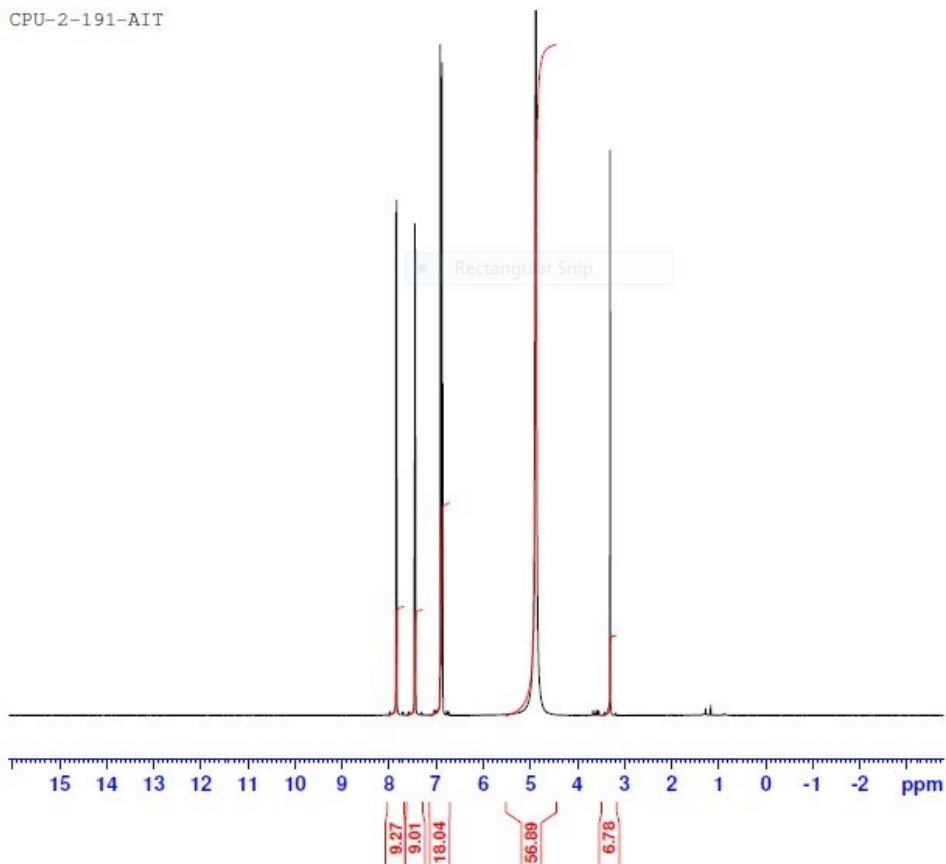
CPU-2-191-AIT

Figure 20. HNMR spectra 2-(2-mercaptobenzoyl)hydrazinecarbothioamide showing chemical shifts.

Table 5. The thermodynamic parameters of NdHL1 determined using the Coats-Redfern model.

Phase	T(k)	K(min^{-1})	t $_{1/2}$	Ea(kJmol^{-1})	ΔH(kJmol^{-1})	ΔS(Jmol^{-1})	ΔG(kJmol^{-1})
Dehydration	703	0.0014	495	33.1	27.2	-243.8	198.6
Decomposition	823	0.0225	30.8	54.7	47.9	-230.9	237.8
Condensation	1123	0,166	4.175	12.7	3.4	-243.3	276.6

Table 6. The thermodynamic parameters of NdHL2 determined using the Coats-Redfern model.

Phase	T(k)	K(min^{-1})	t $_{1/2}$	Ea(kJmol^{-1})	ΔH(kJmol^{-1})	ΔS(kJmol^{-1})	ΔG(kJmol^{-1})
Dehydration	513	0.0022	315	15.1	10.8	-298.5	164.0
Decomposition	673	0.042	16.5	33.9	28.3	-257.8	201.8
Condensation	1123	0.0910	7.641	19.7	10.3	-291.7	337.9

Table 7. The thermodynamic parameters of DyHL1 determined using the Coats-Redfern model.

Phase	T(K)	K(min^{-1})	t $_{1/2}$	Ea(KJmol^{-1})	ΔH(KJmol^{-1})	ΔS(Jmol^{-1})	ΔG(KJMmol^{-1})
Dehydration	513	0.0016	433.125	21.2	17.0	-283.4	162.3
Decomposition	673	0.028	24.75	46.7	41.1	-235.0	199.3
Condensation	1123	0.0769	9.012	28.1	18.7	-281.3	334.6

4.7. X-ray diffraction analysis

The powder X-ray diffraction pattern of the lanthanide complexes were studies using the powder samples at 2-theta degree. Figure 25 to 28 show the XRD pattern of the complexes. The X-ray diffraction pattern of the complexes was indexed using the trial & error method. The interplanar spacing, d, was determine from the diffractogram using the Bragg's equation;

$$d_{\text{hkL}} = \frac{\lambda}{(\sin 2\theta)}, \tag{1}$$

where λ is the x-ray wavelength and θ is half of, the crystallite

Table 8. The thermodynamic parameters of DyHL2 determined using the Coats-Redfern model.

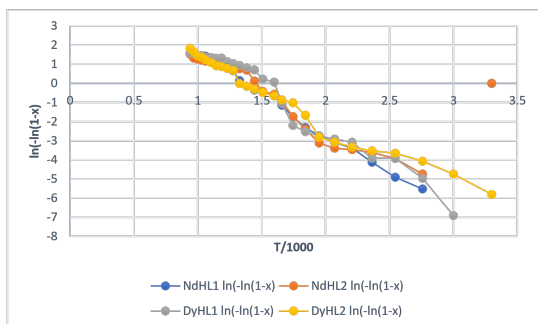| Phase	T(K)	K(min^{-1})	t $_½$	Ea(KJmol^{-1})	ΔH(KJmol^{-1})	ΔS(Jmol^{-1})	ΔG(KJMmol^{-1})
Dehydration	513	0.0022	315	54.3	50.6	-197.5	140.0
Decomposition	673	0.0696	9.957	33.8	28.2	-262.9	205.1
Condensation	1123	0.2277	3.043	26.5	17.2	-280.6	332.3

Figure 21. TGA degradation curves of Dy (III) and Nd (III) complexes of the ligands, HL1 and HL2.
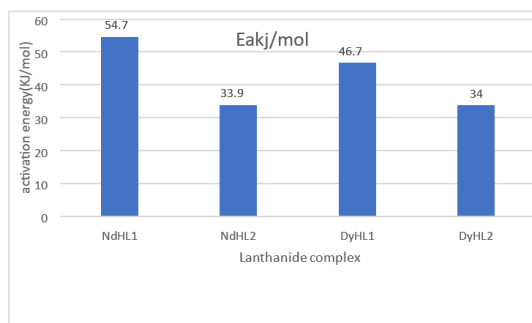
Figure 22. Thermal decomposition activation energy profile of Dy (III) and Nd (III) complexes of the ligands, HL1 and HL2.
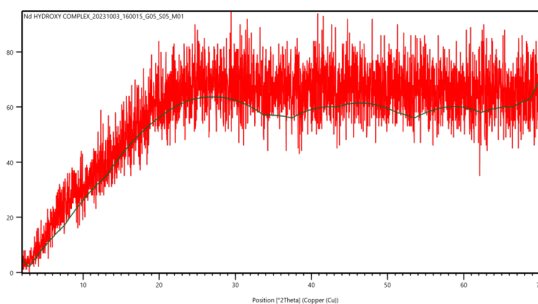
Figure 23. Powder X-ray diffraction spectrum for Nd complex of 2-(2-hydroxybenzoyl)hydrazinecarbothioamide.

size was determined using the Bragg's law

$$D = \frac{0.9}{\beta \cos\theta},$$ (2)

where β is full width at half maximum of diffraction peak (FWHM) [31].
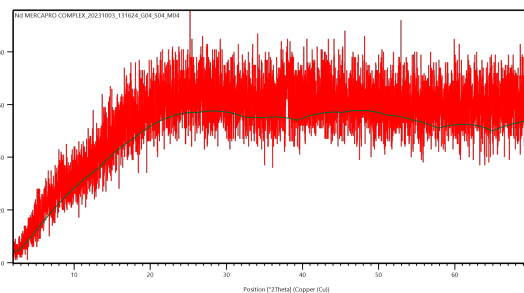
Figure 24. Powder X-ray diffraction spectrum for Nd complex of 2-(2-hydroxybenzoyl)hydrazinecarbothioamide.
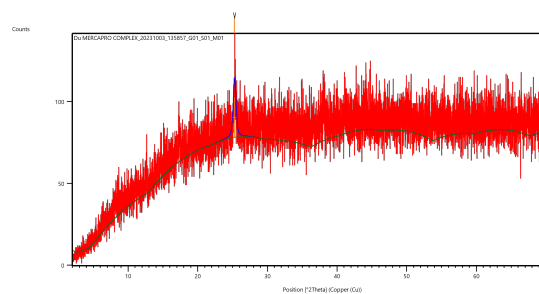
Figure 25. Powder X-ray diffraction spectrum for Dy complex of 2-(2-hydroxybenzoyl)hydrazinecarbothioamide.
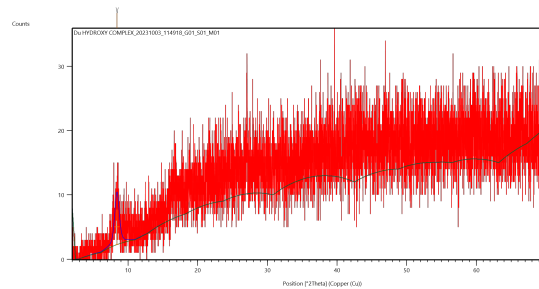
Figure 26. Powder X-ray diffraction spectrum for Dy complex of 2-(2-mercaptobenzoyl)hydrazinecarbothioamide.

4.8. X-ray diffraction studies

The X-ray powder diffraction characterization was carried out using Rigaku Mini Flex600 Japan.

4.9. Antifungal analysis

The antifungal activity of compounds was tested using potato dextrose agar medium, against *A.flavus* by filter paper disc technique. The concentration of test compounds was 12.5μg/ml, 25 and 50μg/ml. After 48hrs of treatment, zones of inhibition produced by all compound were measured in mm.
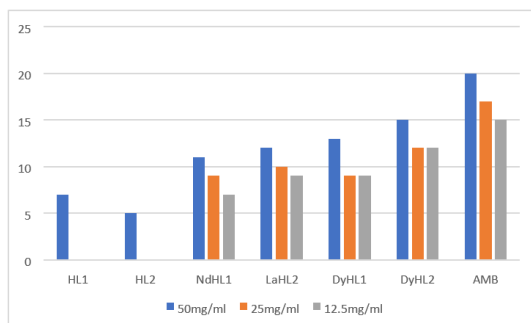
Figure 27. Biological activity of the ligands and their metal complexes against a standard.
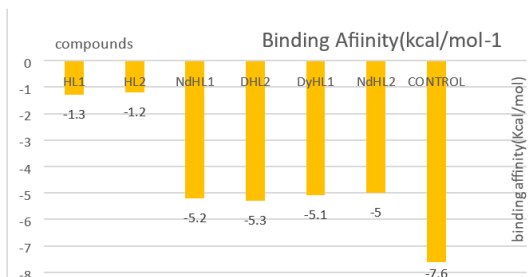
Figure 28. Binding affinity of the ligands and their lanthanide (III) complexes.

Amphotericin-B was used as the standard antifungal agent and DMSO as a control. All the tested compounds showed significant antifungal activity.

4.10. Molecular docking protocol

For the purpose of this study, Aspergillus flavus protein (protein-4c41) was obtained from Protein Data Bank (PDB) at www.rcsb.org. Protein-ligand interacts through intermolecular forces of attraction coexisting between them: hydrogen bound, van der Waals forces of attraction and other related intermolecular forces (Elangovan & Sowrirajan,2022; Delano,2002). The target protein-4C41 was observed to have A:ASN:238 as its key active site. The protein-4C41 was then prepared using Biovia Discovery Studio 2021 by deleting water molecule, defining binding site, the subsequent deletion of the native ligand and the addition of polar hydrogen to enhance the binding. The ligands HL1, HL2, HL3 and the metal complexes were all sketched using ChemDraw-15.1.0.144 and the energy optimized using Chem 3D-15.1. Additionally, the prepared proteins and ligands were docked in AutoDock Tools- 4.2 The 2D structures were visualized using the Biovia Discovery Studio 2021, while the 3D structures of the complexes were visualized using the Py-Mol App.

5. Results and discussion

The coupling of 2-substituted benzoic acids to thiosemicarbazide has been successfully achieved without the use of coupling agents to and at a pH of 7.6. Figures 3 and 4 show the

reaction schemes for the synthesis. The use of coupling agents makes the synthesis cumbersome and capital intensive. The ligands formed complexes rapidly with Nd (III) and Dy (III) metal ions indicating that they are suitable for the extraction of lanthanides from solution. This rapid reaction with the lanthanide ion is desirable since researchers have been in search of suitable ligands for the extraction of rare-earth metals [15]. The action of the ligands is further confirmed by the presence of atoms carrying electron pairs as the ligands meet perfectly some of the most important criteria as extractants for rare each metal. The presence of O, N and S groups in the ligands stand them out as suitable candidates extractants for rare-earth metals. The complexes were studied using thermal and x-ray diffraction techniques. The complexes exhibited thermal stability, cubic structures and higher coordination numbers and are of the general formula $[Ln(HL)_2(H_2O)_m(NO_3)_n](H_2O)_m (NO_3)_n$, where m is equal to 0, 1 or 2 and n is 0 or 1. The lanthanide complexes showed higher melting point than the ligands. The complexes were found to be tricapped trigonal prismatic or Bicapped square antiprism.

5.1. Physical characterization and analytical studies

Table 2 shows the physical and analytical data of the metal complexes. DyH_2 gave the highest melting point, (300 ^{0}C) and the most stable complex compared to other complexes. $DyHL_2$ was formed with the highest yield of 85% compared to other complexes. Figures 1 and 2 show the structures and names of the synthesized ligands. Figures 5 to 8 show the structures of the lanthanide (III) complexes synthesized from the ligands.

5.2. Molar conductivity

The molar conductivity data of the complexes are shown in Table 2 and further confirm the structures of the complexes. The molar conductivity values the lanthanide complexes in DMSO indicate that the complexes are electrolytic in nature except Dysprosium complex of HL1, confirming a coordination number of 9 for the complexes except for the dysprosium complex of HL2. This is in agreement with what is found in the literature for Nd and Dy elements [32]. The range of the values from 112-147 Ω^{-1} cm^2 mol^{-1} agrees with the reports by Ali *et al.* [33] and Ajilounu *et al.* [34]. The molar conductivity values show a 1:2 metal-ligand ratio.

5.3. Electronic spectroscopy

The UV-visible absorption bands of the ligands and their lanthanide complexes were listed in Table 3 as scanned at 1 x 10^{-3}m in DMF. Figure 9 shows the UV-visible spectral of the ligands HL_1 and, HL_2 compared with the complexes. The ligands show strong absorption band in the ultraviolent region. The ligands show maximum absorption between 315 nm and 400 nm. These bands can be assigned to the absorption of the carbonyl group [35]. The bands are arising from the π to π* transition within the aromatic ring and n to π* of the carbonyl functional group. The 2–(2–hydroxybenzoyl) hydrazinecarbothioamide ligand showed maximum absorption of 3.21, at
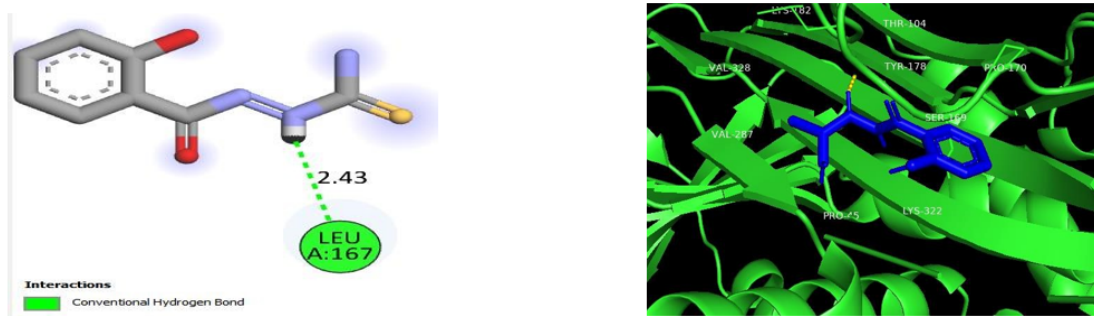
Figure 29. (a) molecular docking of HL1 ligand 2-(2-hydroxybenzoyl)hydrazinecarbothioamide HL1@4C41 (b) 3D structure of HL1 ligand 2-(2-hydroxybenzoyl)hydrazinecarbothioamide against A.flavus protein HL1@4C41
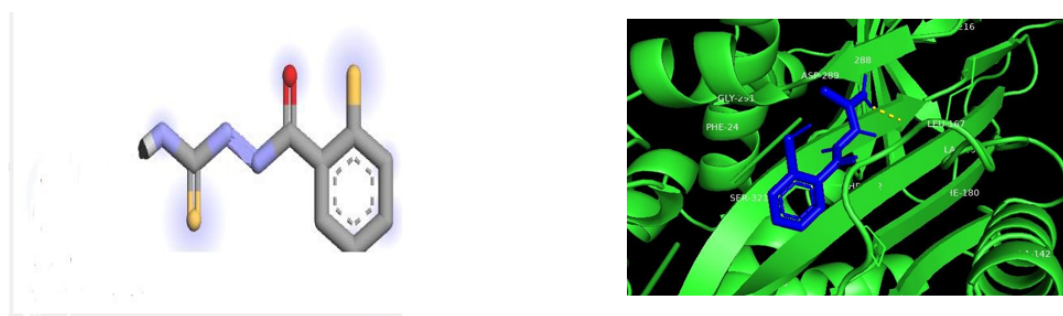

Figure 30. (a) molecular docking of 2-(2-mercaptobenzoyl)hydrazinecarbothioamide (b) 3D structure of HL2 ligand against A.flavus protein HL2@4C4
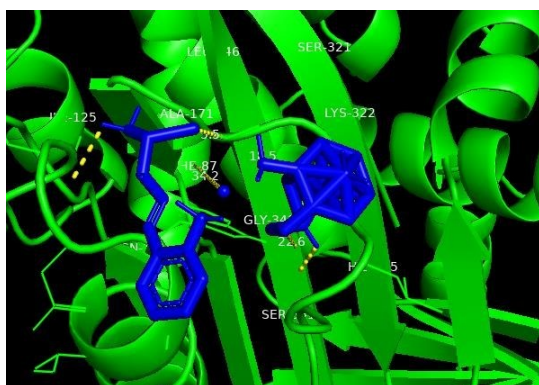
Figure 31. Molecular docking structure of Neodymium complex of HL1 and 2@4c41 protein.
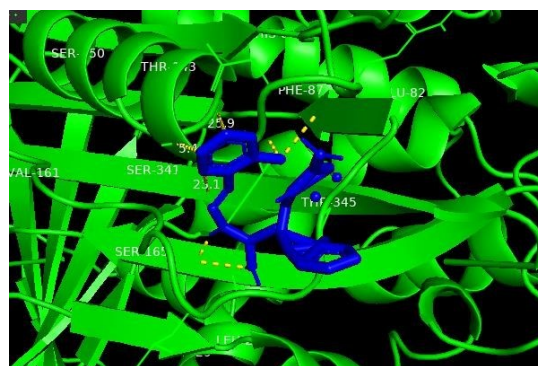
Figure 32. M olecular docking structure of Neodymium complex of HL1 and 2@4C41 protein.

315 nm (3175 cm^1). The ligand also showed significant absorptions of 310, and 335 nm. These bands are shifted to higher frequency in the lanthanide complexes confirming the formation of metal complexes with the lanthanide ions. The 2-(2- mercaptobenzoyl)hydrazinecarbathioamide ligand showed maximum absorption of 0.200 at 412 nm. The bands are shifted to lower wavelengths in the lanthanide complexes indicating the formation of lanthanide complexes with the ligand.

Generally, all the lanthanide complexes, of the two ligands Nd (III) and Dy (III) showed blue shift in the absorption bands of the ligands, as shown in Figure 9. Figure 9 presents clearly

the shift in absorption to a higher absorbance due to complexation. The sharp absorption bands observed for these complexes maybe is attributed to the 4f elections of the lanthanide metals. The molar absorptivity of the complexes (1.0x10^{-4}) indicate charge transfer absorption rather than f-f transfer transition. The higher energies indicate a ligand to metal charge transfer absorption, LMCT, due to ε values of the complexes, 1x10^{-4} molecm^{-1}.The Neodymium (III) complexes of the ligands showed maximum absorbances of 10.00, at 294, 294 and 280nm. The Nd (III) complexes show significant absorption at other wavelengths, as indicated in Table 3. Again, the multi-
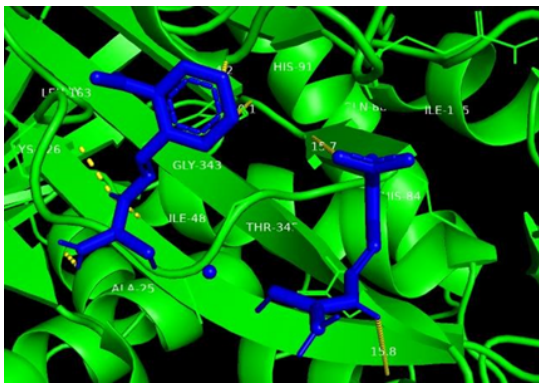
Figure 33. Dysprosium complex of HL1 and 2@4c41 receptor: 4C41.
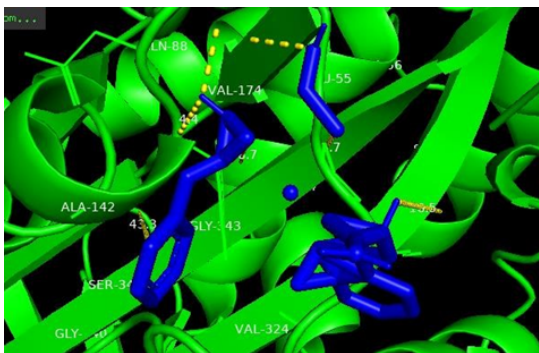
Figure 34. 3-D structure of Dysprosium complex of HL1 and 2@4c41 receptor: 4C41.

ple bands observed for the Nd(III) complexes of the two ligands is attributed to the 4f orbital electrons. The blue shift of the complexes corresponds to 34014 cm^{-1}. 33898cm^{-1} and 35714 cm^{-1}. The molar absorptivity of the complex (10×10^{-4} mole^{-1}cm^{-1}) showed ligand to metal charge transfer absorptions, LMCT. The LMCT absorption behavior of the lanthanide complexes positions the complexes as important compounds for the development of novel materials for LED and displaying technology, lanthanide probes and sensors, photocatalysts and photosensitizers for solar cell, drug delivery and tracking for real-time monitoring of drug and release, oxidation catalysts. They can also find applications in environmental monitoring for detection of metal ion and small molecules in water or air in energy, in energy transfers and enhance optical properties of material in and in biomedical applications.

The Dy (III) complexes of the ligands showed maximum absorbance's of 6.160, 10.00 and 5.220 for (Dy(C$_8$H$_9$N$_3$O$_2$S), (Dy C$_8$H$_9$N$_3$OS$_2$) and (Dy C$_8$H$_{10}$N$_4$OS) at 303, 328 and 303 respectively. The bands appear as single bands which is attributed to complexation reaction [35]. The blue shifts correspond to 33003cm^{-1} and 30488cm^{-1} in HL1 and HL2 respectively.

The absorption of the ligands in the visible and near visible region is crucial especially for a wide range of applications in technology, science, medicine and industry. This suggest that the ligands can undergo photochemical reactions, which are important in processes such as photodynamic therapy and photosensitized reactions. The ligands absorption

behaviors also position them as candidates for the development photo-responsive materials, photocatalysts, organic photovoltaics (OPV), organic light emitting diodes (OLEDs) used in flexible and light weight electronic devices, organic UV-filters, environmental monitoring and sensors, as dyes, pigment and inks in printing and textile materials. The ligands and their dysprosium and neodymium complexes are potential compounds in the development of advanced material for innovative solutions to environmental and industrial challenges.

The blue shift observed in the complexes to wavelengths in the near visible to ultraviolet regions shows increase in transition energy for electrons to move the from the lowest unoccupied molecular orbital to the highest occupied molecular orbital (LUMO to HOMO). The blue shift indicates increase in ligand to metal charge transfer, LMCT energy or ligand -center transitions. This implies increased ligand field and stability of the complexes, increased electron delocalization which will lead to reduction in structural fluctuation and increase stability.

The absorption of LaHL$_2$ complex in near visible region indicate that the transition is due to charge transfer transition. This suggests that the complex has potential catalytic property, especially in photochemical reactions and can be used in the development of dye sensitized solar cells. Absorption in the UV region by the lanthanide (III) complexes indicates that the electronic transitions in the complexes are between molecular orbitals as ligand to metal, LMCT, charge transfer transitions and are potential materials in the development of light emitting devices. The LMCT in the chemistry of lanthanide complexes has significant application in numerous areas such as in lighting, imaging and sensing, catalysis and in energy storage, typically in light emitting diodes LED, fluorescent lamps, optical probes and bioimaging, fluorescent immunoassays and DNA detection, luminescence sensors and environmental monitoring, automotive exhaust cleaners, in polymerization processes for efficient electron control. They also find significant applications in security and anticounterfeiting in bank notes, passports and biometric security. Lanthanide complexes with LMCT transition properties are use in advanced optical photonic materials used as solid lasers in industry and military and in non-linear optical devices, NLO used in optical switches and frequency doubling devices.

These absorption properties such as the significant LMCT transition position the lanthanide (III) complexes as potential materials for the development of novel photosensitizers and photovoltaic materials. This enhanced strong LMCT interaction as observed in all the complexes. This ability of the lanthanide complexes to absorb light and participate in charge transfer transition processes makes the complexes suitable materials for solar energy conversion. This is similar to the findings reported by Refs. [36, 37].

5.4. Infrared spectroscopy

The ligands and their Lanthanide (III) complexes were characterized using FTIR spectra. The important FTIR spectral data of the ligands and their lanthanide complexes are presented in Table 4. Figures 13 and 14 show the FTIR spectral of the free ligands HL1 and HL$_2$ respectively. Figures 15 to 18 show the

FTIR spectra of the Nd and Dy complexes of HL1and HL2 ligands.

The IR spectral of the ligands show broad bands at 3336-3108cm^{-1} which are assigned to (N-H) stretching frequencies. The bands appear at 3362 and 3336 for HL$_1$ and HL$_2$ respectively, while the bands appearing at 1654, and 1647cm^{-1} are assigned to v(C=O) of Carbonyl frequencies in the HL$_1$, HL$_2$ and HL$_3$ ligands respectively. The bands at 887-879cm^{-1} in the ligand spectra are assigned to C=S frequencies. The bands at 1043-1151 are assigned to N-N vibration, in the Ligands. The bands in the region 1580 – 1520cm^{-1} observed in the ligands HL1 and HL$_2$ is assigned to the v(N = N) stretching frequency of straight chain azo groups. The bands at 3429 – 3908cm^{-1} in the ligands is assigned to V(O–H) stretching vibrations [38]. This suggests the possible existence of hydrazo azo tautomerism or keto-enol tautomerism. The enol form due to steric hindrance are likely prevented from complexation in preference to the keto form. Hegazy and his coworkers reported similar results [39].

In the lanthanide complexes, the vibrational bands observed in the free ligands and assigned to the amide carbonyl stretching frequency is shifted to a lower frequency in the complexes by 152 – 141cm^{-1} in the lanthanide (III) complexes. This significant shift in the v(C=O) vibration frequency observed in the complexes indicate participation of the oxygen atom of the C=O group in the coordination the v(C=O) frequencies are shifted to lower wavenumber in all the complexes to 1594-1513cm^{-1} for all the lanthanide (III) complexes. The observation of the 3336-3108cm^{-1} frequency range found in the lanthanide complexes spectral confirm that the N-H groups were not involved in the complexation process. The formation of lanthanide (III) complexes was further confirmed by the appearance of new bands at 403-600 cm^{-1} in the spectra of all the lanthanide (III) complexes.

The bands at 402-431cm^{-1} v(453-461cm^{-1} and 510-585cm^{-1} are assigned to v(Ln-N), v(Ln-O) and v(Ln-S) frequencies respectively. The frequencies at 640-663 cm^{-1} in the lanthanide (III) complexes are assigned to coordinated v(O-H) stretching frequencies in the metal complexes. The bands at 1142-1150cm^1 and 1089-975 cm^{-1}in the lanthanide (III) complexes are assigned to v(N-C-N) and (N-N). The bands at 840 – 815 is assigned to v(NO$_3^-$) stretching vibration in the complexes [38].

The suggested geometries of the Dy (III) and Nd (III) complexes of the tetradentate ligands 2-(2-hydroxybenzoyl)hydrazinecarbothioamide,HL1 and 2-(2-marcaptobenzoyl)hydrazinecarbothioamide,HL2 studied were supported by the appearance and absence of specific bands in the various spectra of the complexes. The appearance of bands at 640-657 cm^{-1} in all the Neodymium complexes and the dysprosium complex of HL2 which are assigned to stretching frequency of coordinated water molecule are absent in the FTIR spectra of dysprosium complex of HL1 ligand. This suggests one coordination number higher in all the complexes of neodymium and HL2 complex of dysprosium than the coordination number of dysprosium in HL1 complex. This was further supported by the XRD peaks. The geometries

are further supported by the appearance of bands at 811-820 cm^{-1} in the spectra of all the complexes which are assigned to NO$_3^-$ vibrational frequency which is again confirmed by the results obtained from molar conductivity studies. The molar conductivity values of NdHL1, NdHL2 and DyL2 range from 132 – 147 Ω^{-1} cm^2 mol^{-1} in DMSO which indicate that the complexes conform to electrolytic 2:1 ligand -metal ratio complexes according to Ali *et al.* [33]. The molar conductivity value of 32 Ω^{-1} cm^2 mol^{-1} obtained for dysprosium complex of HL1 suggests that the complex is a non-electrolytic with 2:1 ligand -metal ratio. Table 4 shows the important IR bands OF the Ligands and their Lanthanide complexes in (cm^{-1}).

5.5. Nuclear magnetic resonance spectroscopy

The proton Nuclear Magnetic Resonance (NMR) spectra of the organic compounds were obtained with CDCl$_3$ as solvent. The peaks in the ^{1}HNMR spectra confirmed the bands observed for the ligands in the FTIR spectra and are shown in Figures 14 and 15. The δ-NH, NH$_2$, aromatic protons C=O, are all present in the 1HNMR peaks for the three ligands. For HL$_1$, the peaks appear in the range of 3.33 – 3.41ppm (NH2), 6.810 – 6.822ppm (ArHC-H), 7.36 – 7.38ppm (ArH(CH)), 7.87 – 7.90ppm (NH), and 4.625.0ppm(C=O). For HL$_2$, the peaks appear in the range 3.28-3.30(NH2), 6.815-6.822(ArHC-H),7.447.48(ArH(CH)), 7.88-7.90(NH) and 4.62-5.0(C=O) [40].

5.6. Thermal analysis

Thermogravimetric Analysis (TA) of the lanthanide complexes were carried out within 30 to 850^{0}C using nitrogen inert gas flow condition with a heating rate of 10^{0}C/min. All the lanthanide complexes, showed similarities in thermal decomposition and degradation. The TGA curves of the lanthanide complexes presented in Figures 21 to 24 indicate a three-phase change for all the lanthanide (III) complexes studied. All the complexes, exhibited thermal stability up to 400^{0}C. The first phase degradations varied from one complex to another with 240 ^{0}C being the dominant degradation temperature among the complexes. However, the thermal stability of all the lanthanide complexes varied among them.

First degradation occurring in all the complexes was due to loss of water molecule and NO$_3$, except for DyHL$_1$ complexes which took place due to loss of NO$_3$. The average percentage weight loss in the first phase in the complexes is about 3% corresponding to 0.463g. The second phase degradation was due to the loss of ligand mass and the formation of Ln$_2$O$_3$. The TGA Curves for the lanthanide (III) complexes as shown in Figure 21 shows the weight loss during the degradation in three phases due to dehydration, decomposition and condensation reactions in the complexes. The curves are endothermic in nature and can be correlated with thermodynamic parameters [41]. kinetic and thermodynamic parameters were calculated for the three phases for all the complexes using the TGA data. Tables 5 to 8 show the kinetic and thermodynamic parameter determined using the

Coats-Redfern model equation with modification described in equation 3.

$$\ln(-\ln(1-x)) = \ln(ART^2) - \frac{E_a}{\beta E_a/RT}, \qquad (3)$$

where A is pre-exponential factor or frequency factor, β is heating rate (10 c/ min), R is the universal gas constant (8.314Jmo1^{-1} K^{-1}), E_a is activation energy and T is temperature in kelvin. Plotting a graph of ln(1-x) against 1/T for each phase the determination gave values for activation energy determined from slope of the graph using the relation:

$$Ea = slope \times R. \qquad (4)$$

Other parameters were computed using the basic thermodynamic equation [42].

The rate constant and half-life of reactions were determined by considering all the phase transformations as 1st order reactions, given in equation (5) [43, 44].

$$\frac{dx}{dt} = k(1-x), \qquad (5)$$

where

$$x = w_i - w_t w_0, \qquad (6)$$

and wi is the initial weight, wt is weight of sample at particular time, t and w is final weight. Equation (4) can be written as

$$\ln(1-x) = -kt. \qquad (7)$$

The rate constants for the phases were determined by plotting graphs of ln(1-x) against time, t and determining the slope of the graphs which is equal to k according to equation (7).

The straight lines obtained for all complexes confirmed that transformations for different phases for all the complexes were of first order reactions. The slope of each phase graph for each complex gave the numerical value of the rate constant, K for the particular phase for each complex. The half-life, $t_{1/2}$ for each phase was determined using equation (8) substituting the values of k for each phase of each complex

$$t^{\frac{1}{2}} = \frac{0.695}{K}. \qquad (8)$$

The values of the activation energy, of the phases show that the decomposition reaction occurred more slowly followed by the condensation reaction in almost all the complexes except for DyhL$_1$ and DyHL$_2$. This deviation from the observed behavior of the other complexes may be due to the metal playing a catalytic role in the DyhL$_1$ and DyHL$_2$ complexes, thereby lowering the activation energies of the decomposition phases/reaction of the complexes. The activation energies of the decomposition phases of the lanthanide (iii) complexes range from 33809 to 54.7 KJmo1^{-1} at 400 °C, with DyHL$_1$ decomposing at a temperature of about 600 °C which is quite higher than the decomposition temperature of other complexes, followed by DyhL$_1$ and DyhL$_2$ with decomposition temperature of 550 °C. Activation energy, Ea is a function of bond breaking. The higher the values of activation energy, Ea, the harder it is to break the

bonds and hence, the more stable the compound. Figure 21 show the decomposition activation energies of the complexes. The rate constants, k for the decomposition reactions were observed to vary with activation energy, Ea. The higher the values of activation energy, the lower the rate constant, k. This implies that the higher the values of activation energy values, Ea, the slower the rate of the chemical reaction will proceed [45, 46]. The rate c The lanthanide complexes can be arranged in their order of thermal stability to decomposition in the order NdHL$_1$ > DyHL$_1$ > NdHL$_2$ > DyHL$_2$. The positive values of ΔG for all the complexes show that the degradation reactions are non-spontaneous. The ΔH values for all the lanthanide (III) complexes studied were positive. Condensation and decomposition reactions were found to be endothermic reactions, as well as the dehydration reactions. The high values of Ea of the complexes for dehydration and decomposition phases show that the lanthanide (III) complexes are thermally stable [28]. The geometry of the lanthanide complexes can significantly influence the rate constant which is a measure of the ligand exchange rate and the catalytic activities of the complexes. The bicapped square antiprismatic geometry BSA showed higher rate constant which can be attributed to reduced steric hindrance, making the complexes more labile than the tricapped trigonal prismatic, TTP complexes. Which is more rigid. The rate constant of reactions that involve lanthanide complexes can be significantly influenced by other factors such as electronic and ligand effects.

Pre-exponential factor A or frequency factor for the phases were determined using the Coats-Redfern equation from the intercepts of the plot of eqn. (3) and solving for A:

$$A = \frac{\beta E_a 2\exp(I)}{RT}, \qquad (9)$$

where β is the heating rate, 10 ^{0}C/min, where I is the intercept on the ln(1-x) axis, Ea is activation, R is gas constant 8.314 and T is temperature in Kelvin. We observed that the pre-exponential factors A of all the complexes followed a uniform equation given as equation (10) which we found valid for the conditions used for the TGA study which can be employed for a heating rate β of 10 °C/min,

$$A = Ke\frac{E_a}{T^2}\exp(I), \qquad (10)$$

where K$_e$ is constant for all the complexes studied and is given as 0.02005 at heating rate of 10 ^{0}C/min.

The pre-experiential factor, A was used to determine the entropy changes, ΔS and Gibbs free energy changes ΔG for the phases for each complex. Enthalpy change, ΔH was determined using the relation.

$$\Delta H = E_a - RT, \qquad (11)$$

where E$_a$ is activation energy R is gas constant and T is temperature in Kelvin.

The values obtained for pre-exponential factor A$_i$ varied form complex to complex. Pre-exponential factors give insight into the frequency of effective collision and depends on temperature. Activation energy, E$_a$ is important for reaction engineering for modelling and optimization.

The results show that the complexes are crystalline complexes except, $NdHL_1$, and $NdHL_2$ which did not produce peaks, indicating that they could be crystals with small sizes or amorphous compounds. All the complexes of dysprosium with the ligands are crystalline as shown in Figures 25 and 26 which produced peaks. NdHL1 and NdHL2 did not produce peaks as shown in Figures 23 and 24. The crystalline complexes have potential applications in several areas due to their unique optical, magnetic and electronic properties resulting from the presence of lanthanide ions such as in the development of luminescence material, biomedical imaging, fluorescence probe, catalysis, optical devices, sensors, energy conversion, data storage and environmental application while the amorphous complexes due to their unique optical properties are potential compounds in the development of materials such as phosphors in light emitting devices, fluorescence probes, magnetic resonance imaging, MRI, optical data storage system, thin film coating and in environmental remediation due to the adoption and ion-exchange properties of lanthanide complexes. Further controlled synthesis conditions such as hydrothermal synthesis and slow evaporation techniques can improve the crystallinity of the complexes, especially NdHL1 and NdHL2 [47, 48].

5.7. Antimicrobial activity

All the compounds synthesized showed significant antimicrobial activities against the organisms tested. The ligands and their lanthanide (III) complexes showed more activities against fungi. The lanthanide complexes exhibited higher biological activities against the organisms more than the ligands. This agrees with the findings reported by Ajilouni *et al.* [49] and Tharkur [50].

Aspergillosis has been reported as a co-infection in the recent times [51, 52]. Fungal infections have been reported to increase during the covid-19 outbreak due to their attack on immune system thereby weakening the body's defense system [53–55]. A number of symptoms are known to be related to aspergillosis which include stiffness, cough with blood, pain, running nose, fever, etc [52]. Aspergillus flavus is a well-known pathogenic fungus that has the potential to produce aflatoxins that are toxic and highly carcinogenic. Amphotericin-B was used as standard antifungal drug and DMSO used as control [56, 57]. The results show that the complexes compete favorably with the anti-fungal standard drug, amphotericin-B, used for the study, the most biologically active complex DyHL2 with 15mm at 50mg/ml compared to the 20 mm inhibition observed for the standard drug AMB used for the study. This implies that the complexes are potential compounds for the development of anti-fungal drugs when compared with the free ligands. This result was further confirmed by molecular docking studies, where the ligands, HL1 and HHL2 gave binding affinity of -1.3kcal/mol and -1.2 kcal/mol respectively compared to -5.2 kcal/mol, -5.3 kcal/mol, -4.9 kcal/mol, -5.1 kcal/mol and -5.0 kcal/mol for their lanthanide complexes. The enhanced biological activity exhibited by the lanthanide (III) complexes compared to the free ligands can be attributed to the increased membrane permeability and cell up take. Lanthanide complexes exhibit higher lipophilic properties than free ligands. This increases the interaction of the complexes with intercellular targets more than in the free ligands, which will lead to more effective activity as observed. Other factors. The enhanced biological activities of the lanthanide complexes can also result from alteration of ligand electronic properties due to complexation, generation of reactive oxygen species, ROS, increased binding to biomolecules, chelation and synergistic effects. These properties make the complexes potential materials for the development of new antimicrobial agent. Molecular docking studies, a computational approach to ligand-protein target docking technique has been applied in the study of chemical and structural properties of the ligand receptor complex. Molecular docking has been a useful tool in computational studies and drug discovery [58–60]. Figure 27 shows the biological sensitivity of the ligands and their lanthanide (III) complexes. The result shows that the metal complexes unlike the ligands compete favorable as alternative pharmacological replacement for Amphotericin-B used as a standard drug as indicated in Figure 27.

5.8. Molecular docking studies

Molecular docking studies was carried out in other to comprehend the mechanism by which ligands recognize the specific active poses in a protein since each protein have numerous active sites, the Aspergillus flavus protein obtained was docked against the compounds, their likelihood to bind to the metal complex was obtained. Hence the result of the docking analysis is presented in Figure which displays a good binding ability of the ligand to the target protein. Amphotericin-B was used as antifungal drug for the study. Aspergillus flavus is a known common saprotrophic and pathogenic fugus with is distributed globally. This fungus is known for its common establishment of infection legumes, grains and tree nuts. Aspergillus flavus is lately known for its ability to cause keratitis, granulomatous sinusitis, wound infection in human, which requires developing novel therapeutic drug [61].

Understanding strong binding affinity and important conventional hydrogen bonds is a more vital resources for identifying effective interaction of the proposed drug and the target protein [61, 62]. The HL_1 and HL_2 compounds achieved their optimal positioning with binding affinities (best pose) of -1.3kcal/mol and -1.2 kcal/mol respectively. Whereas the best pose of the metal complexes are -5.2 kcal/mol, -5.3 kcal/mol, -4.9 kcal/mol, -5.1 kcal/mol and -5.0 kcal/mol for neodymium complexe-1@4c41, disprosium complexe-2@4c41, Neodymium complex-1@4c41, Neodymium complex-2@4c41, Dyspeosium complex1@4c41 and Dyspeosium complex-2@4c41 respectively as presented in Figure 28. From the result obtained it is clearly seen that dysprosium complexe-2@4c41 has the highest binding affinity with -5.3 at its best pose as presented in Figure 28. compared with other complexes, this shows that dysprosium complexe-2@4c41 is more effective at inhibiting the target protein. Hence this can be best interpreted as Dyspeosium complex2@4c41>Dyspeosium complex-1@4c41> Neodymium complex-1@4c41> Neodymium complex2@4c41>HL1@4c41> HL2@4c41 and HL2@4c41

in terms of their respective inhibitory potential as represented in Figure 28. Consequentially, Figures 29 and 30 show that HL1and HL2 show less conventional hydrogen bonds than the complexes Neodymium complex-1, Neodymium complex-2, Dyspeosium complex-1 and Dyspeosium complex-2 respectively. The Lipinski rule of five also predicts that compounds with more than five hydrogen-bond acceptors will have poor absorption or penetration properties. These complexes interacted with the protein and in accordance to the Lipinski rule of five, the complexes result in not less than five hydrogen-bound interactions with crucial amino acid residues together with their corresponding bond distances in Å as shown in Figures 31 to 34 in 3D, whereas, the ligands formed less than five hydrogen bond-acceptors which makes them a better pharmacological alternative in obedience to the Lipinski rule of five as presented in Figures 29 and 30. The result of this study is of the notion that dysprosium complex of HL2 complexe-2 will be more effective pharmacological option compared with the other compounds studied for Aspergillus flavus therapy in terms of the binding affinity whereas in obedience to the Lipinski rule of five the HL_1 and HL_2 will serve as a preferred pharmacological option for, Aspergillus flavus disease treatment due to their low molecular weight. The Lipinski rule of five provides that low molecular weight compounds will bind more effectively than molecules with high molecular weight such as the lanthanide complexes. This agrees with the results obtained with the in vivo studies of the compounds. 2D and 3D visualization showing interactions between ligand and amino acid residues of Aspergillus flavus proteins (distance in Å). The higher binding affinity of DyHL2 compared to the other complexes can be attributed to stronger ligand donor bond effects in the complex which will enhance its binding affinity compared to the other complexes. The coordination geometry, chelation and steric factors can contribute to the higher binding affinity observed for DyHL2 resulting from the ligand's optimal spatial arrangement around the Dy^{3+}, which will lead to orbital overlap and result to stronger bonding. The lower activation energy value,34 $kJmol^{-1}$ for DyHL2 compared to the other complexes implies lower kinetic stability which will favor bonding with biomolecules and lead to stronger bonding and higher binding affinity compared to the other complexes with higher activation energies.

5.9. Pymol visualization of the ligands and Aspergillus flavus protein

Molecular docking studies, a computational approach to ligand-protein target docking technique has been applied in the study of chemical and structural properties of the ligand-receptor complex. Molecular docking has been a useful tool in computational studies and drug discovery [63–67].

Considering the structures of the complexes and their biological activities, their thermal stability and absorbance within the UV Visible and near infrared region, they can find diverse applications across multiple fields including drug discovery such as in the development of new antibiotics, deep imaging and photothermal therapy. This is following their enhanced biological activity compared to the free ligands. The amorphous complexes, NdHL1 and NdHL2 can find application as photocatalysts in CO2 catalytic degradation and water splitting which can contribute to hydrogen production and aiding in environmental remediation. The Dy^{3+} complexes with high UV absorption are potential materials for protective coatings for solar panels and optical lenses to prevent UV induced degradations and in high performance laser glasses and UV-blocking films for aerospace applications. They can be used in LED and OLED displays offering stable and efficient light emission and in laser materials widely used in industrial cutting, telecommunication and medical laser systems, single molecule magnets, SMMs and quantum computing and ultra-high-density storage [68, 69]. The authors suggest the use of mixture of ethanol and water in a ratio of 70: 30 for the recrystallization of the complexes. This to allow the formation of higher quality crystals.

6. Conclusion

The design and synthesis of new hydrazinecarbothioamide derivative compounds were carried out using Chemdraw ultra slim 12 version by Harvard and synthesized in the laboratory. The coupling of 2substituted benzoic acids to thiosemicarbazide has been successfully achieved without the use of coupling agents. The compounds were characterized using spectroscopic and physical methods. The complexes were characterized using spectroscopic, thermal and x-ray diffraction studies. The complexes exhibited thermal stability and higher coordination numbers and of the general formula $[Ln(HL)_2(H_2O)_m(NO_3)_n](H_2O)_m(NO_3)_n$, where m is equal to 0,1 or 2 and n is 0 or 1. The lanthanide complexes showed higher melting point than the ligands. The complexes were found to be tricapped trigonal prismatic or Bicapped square antiprism. Both the synthesized ligand and their lanthanide (III) complexes showed significant antimicrobial activities against aspergillus flavus and demonstrated potentials as drug precursors for the synthesis of antimicrobial agents and in the development of novel imaging and sensing agents. agents. The electronic, thermal stability and X-ray diffraction studies show that the complexes are potential materials for the development of photosensitized materials and photo cell as well as photocatalysts and significant application as sensing and imaging. The ligands formed complexes rapidly with Nd (III) and Dy (III) metal ions indicating that they are suitable for the extraction of lanthanides from solution. This rapid reaction with the lanthanide ion is desirable since researchers have been in search of suitable ligands for the extraction of rare-earth metals. The action of the ligands is further confirmed by the presence of atoms carrying electron pairs as the ligands meet perfectly some of the most important criteria as extractants for rare each metal. The presence of O, N and S groups in all the ligands stand them out as suitable candidates extractants for rare-earth metals. Molecular docking studies revealed that the ligands and all their metal complexes are pharmacological alternatives for the treatment of aspergillus flavus. Applications of the complexes in photocatalysis is desirable to determine their effectiveness as photocatalyst. Furter studies on the anti-oxidant and anti-cancer activities of these ligands and their metal complexes will go further

to establish the biological potentials of these compounds and their applications in the development of new drug agents. The complexes have demonstrated potential as photocatalysts and should studied for their photocatalytic efficiency in the organic transformations.

Data availability

The data used in this study is available upon reasonable request.

References

[1] P. W. Seavill & J. D. Wilden, "The preparation and applications of amides using electrosynthesis", Green Chem. **22** (2020) 7737. https://doi.org/10.1039/D0GC02976A.

[2] X. Zhang, T. X. Cui, X. Zhao, P. Liu & P. Sun, "Electrochemical difunctionalization of Alkenes by a four-component reaction cascade mumm rearrangement: rapid access to functionalized Imides", Angew. Chem. **59** (2020) 3465. https://doi.org/10.1002/anie.201913332.

[3] D. Çanakçi, "Thermal stability, degradation kinetic and structural characterization of novel aromatic amide compounds", Journal of Molecular Structure **1205** (2020) 127645. https://doi.org/10.1016/j.molstruc.2019.127645.

[4] U. B. Amadi, M. O. C. Ogwuegbu, C. K. Enenebeaku & G. O. Onyedika, "A Review on synthesis, lanthanide complexes and biological activites of hydrazone derivatives of hydrazinecarbothioamides", International Research Journal of Pure and applied chemistry **24** (2023) 54. https://doi.org/10.9734/irjpac/2023/v24i5825.

[5] A. A. Al-Amiery, Y. K. Al-Majedy, H. H. Ibrahim & A. A. Tamimi, "Antioxidant, antimicrobial, and theoretical studies of the thiosemicarbazone derivative Schiff base 2-(2-imino-1-methylimidazolidin-4-ylidene)hydrazinecarbothioamide (IMHC)", Org Med Chem Lett. **2** (2012) 4. https://doi.org/10.1186/2191-2858-2-4.

[6] A. A. Al-Amiery, A. A. H. Kadhum., B. Mohamad, & S. Junaedi, "A novel hydrazinecarbothioamide as a potential corrosion inhibitor for mild steel in HCl", Materials **6** (2013) 1420. https://doi.org/10.3390/ma6041420.

[7] T. Darell, S. T. Hulushe, T. E. Mtshare, M. R. Beteck, M. Isaacs, D. Laming, H. Hoppe, R. W. M Krause, & S. Khanye , "Synthesis, antiplasmodial and antitrypanosomal evaluation of a series of novel 2-Oxoquinoline-based Thiosemicarbazone derivatives", Afri. J. Chem. **71** (2018) 174. https://doi.org/10.17159/0379-4350/2018/v71a23.

[8] N. U. Guzeldemirci, S. Cimok, N. Das-Evcimen, & M. Sarikaya , " Synthesis and aldose reductase inhibitory effect of some new Hydrazinecarbothioamides and 4-Thiazolidinones bearing an Imidazo[2,1-*b*]Thiazole moiety", Turk. J. Pharm. Sci. **16** (2019) 1. https://doi.org/10.4274/tjps.05900.

[9] A. A. Hassan, R. Yusria, Y. I. Ibrahim, E. M. El-Sheref, & S. Bräse, "Novel synthesis of 1,3-Thiazine and Pyrimidinethione derivatives from (1-Aryl ethylidene)hydrazinecarbothioamides and Tetracyanoethylene", J. Heterocyclic Chem. **53** (2016) 876881. http://dx.doi.org/10.1002/jhet.2350.

[10] M. A Bhat, A. A. Khan, H. A. Ghabbour, C. K. Quah & H. Fun, "Synthesis, characterization, x-ray structure and antimicrobial activity of N-(4-chlorophenyl)-2-(pyridin-4-ylcarbonyl) hydrazinecarbothioamide", Trop. J. Pharm. Res. **15** (2016) 1751. http://dx.doi.org/10.4314/tjpr.v15i8.22.

[11] A. A.Hassan, A. A. Aly, N. K. Mohamed, K. M. El- Shaieb, M. M. E. Makhlouf, E. S. M. Abdelhafez, S. M. Bräse, K. N. Nieger & T. S. Kaoud, "Design, synthesis, and DNA interaction studies of furo-imidazo [3.3. 3] propellane derivatives: Potential anticancer agents", Bioorg. Chem. **85** (2019) 585. https://doi.org/10.9734/irjpac/2023/v24i5825.

[12] A. Aly , A. A. Hassan, S. M. Abdal-latif , M. A. A. Ibrahim, S. Brase & M. Nieger, "Reaction of N,N'-disubstituted hydrazinecarbothioamides with 2-bromo-2-substituted acetophenones", Arkivoc. **23** (2013) 102. https://doi.org/10.24820/ark.5550190.p010.385.

[13] A. A. Hassan, A. A. Ashraf, T. I. M. Bedair, A. B. Brownn, I. Talaat & T. I. A. El-Emary, "Facile method for the synthesis of hydrazine-4-oxothiazolidine and imino-5-oxothiadiazine derivatives from 1,4-disubstituted thiosemicarbazides", Journal of Heterocyclic Chemistry **51** (2013) 44. https://doi.org/10.1002/jhet.1655.

[14] S. J. Allison, G. P. Ashton, H. J. Lynch, B. R. Shire, R. M. Phillips, G. M. B. Parkes, E. Pinder, C. R. Rice, A. A. M. Teixeira, T. Volleman & D. A. Wordsworth, "Preclinical Evaluation of Zn(II) Self-Assemblies with Selective Cytotoxic Activity Against Cancer Cells In Vitro and *In Ovo*", Chem. Eur. J. **30** (2024) 1. https://doi.org/10.1002/chem.202302803.

[15] N. A. Ismail, M. A. AZIZ, Y. M.Yunus & A. Hisyam, "Selection of extractant in rare earth solvent extraction system: A review", international journal of recent technology **8** (2019) 2277. http://umpir.ump.edu.my/id/eprint/25038.

[16] J. G. Bunzli, "Review: Lanthanide coordination chemistry: from old concepts to coordination polymers", J. Coord. Chem. **67** (2014) 3706. https://doi.org/10.1080/00958972.2014.957201.

[17] A. Carac , "Biological and biomedical applications of the lanthanides compounds: A Mini Review", Proc. Rom. Acad. **19** (2017) 69. https://academiaromana.ro/sectii2002/proceedingsChemistry/doc2017-2/art01.pdf.

[18] F. B. Tamboura, A. Gueye, P. A. Gaye, M. Diallo, N. Gruber, A.Joualti & M. Gaye, "Dinuclear lanthanide(iii) complexes withschiff bases ligands derived from carbonohydrazide. Synthesis, spectroscopic studies and structural characterization", Journal of Applied Chemistry **12** (2019) 2278. https://doi.org/10.9790/5736-1210015967.

[19] K. Raja, A. Suseelamma & K.Reddy, "Synthesis, spectral properties and DNA binding and nuclease activity of lanthanide (III) complexes of 2-benzoylpyridine benzhydrazone: X-ray crystal structure, Hirshfeld studies and nitrate-π interactions of cerium(III) complex", J. Chem Sci. **128** (2016) 23. https://doi.org/10.1007/s12039-015-1003-y.

[20] M. H. Al-Amery, B. Al-Abdaly & M. K. Albayaty, "Synthesis, characterization and antibacterial activity of new complexes of some lanthanide ions with 15-crown-5 and 18-crown-6", Orient. J. Chem. **32** (2016) 1025 . http://dx.doi.org/10.13005/ojc/320228.

[21] N. M. Sudhindra, M. A. Gagnani , D. M. Indira & R. S. Shukla, "Biological and clinical aspects of lanthanide coordination compounds", Journal of Bioinorganic Chemistry and Applications **2** (2004) 159. https://doi.org/10.1155/S1565363304000111.

[22] M. S. Iorungwa, J. A. Atagheri, P. T. Shimaibo & V. J. O. Nane, "Synthesis, characterization and biological profiles of Schiff base aldimines derived from N-N1- Diphenyl-O-Pyrol-6-Methyleneacetate and its Cu^{2+} and Fe^{2+} complexes" Advanced Journal of chemistry Research **1** (2023) 29. https://doi.org/10.31248/AJCR2023.006.

[23] R. K. Sodhi, S. Paul, R. K. Sodhi & S. Paul, "Metal complexes in medicine an overview and update from drug design perspective" Cancer Therapy & Oncology International Journal Cancer Therapy & Oncology International Journal **2** (2019) 001. https://dio.org/10.19080/CTOIJ.2019.14.555883.

[24] A. Gola, T. Knysak, I. Mucha & V. Musial, "Synthesis, thermogravimetric analysis, and kinetic study of Poly-*N*-Isopropylacrylamide with varied initiator content", Polymer **15** (2023) 2427. https://doi.org/10.3390/polym15112427.

[25] A. Z. Sarsenbekova, G. M. Zhumanazarova, Y. M. Tazhbayev, G. K. Kudaibergen, S. K. Kabieva, Z. A. Issina, A. K. Kaldybayeva, A. O. Mukabylova & M. A. Kilybay, "Polymer (Basel)", Research the thermal decomposition processes of copolymers based on polypropyleneglycolfumaratephthalate with acrylic acid", polymers **15** (2023) 1725. https://doi.org/10.3390/polym15071725.

[26] F. I. Chiriac, M. Ilis, A. Madalan, D. Manaila-Maximean, M. Sech & V. Circu, "Thermal and emission properties of a series of lanthanides complexes with *N*-Biphenyl-Alkylated-4-Pyridone Ligands: crystal structure

of a terbium complex with *N*-Benzyl-4-Pyridone", Molecules **26** (2021) 2017. http://dx.doi.org/10.3390/molecules26072017.

[27] M. R. Mahendrasinh, V. P. Hermal, M. R. Lata & K. P. Nayarika, "Synthesis and biological evaluation of 1,3,4-thiadiazole analogues as novel AChE and BuChE inhibitors" International Journal of Pharmacy and Bioscience **3** (2023) 814. https://doi.org/10.1016/j.ejmech.2012.12.060.

[28] G. Singh, V.Tyagi, P. Singh & A. Pandey, "Estimation of thermodynamic characteristics for comprehensive dairy food processing plant: An energetic and energetic approach", Energy **194** (2020) 116799. https://doi.org/10.1016/j.energy.2019.116799.

[29] A. Falco, M. Neri, M. Merigari, L. Baraldi, G. Bonfant, M.Tegoni, A. Serpe & L. Marchio, "Semirigid ligands enhanced different coordination behavior of Nd and Dy relevant to their separation and recovery in a non-aqueous environment", Inorg. Chem. **61** (2023) 16110. https://doi.org/10.1021/acs.inorgchem.2c02619.

[30] W. Chan, C. Xie, W. Lo, J. G. Bunzli, W. Wong & K. Wong, "Lanthanide tetrapyrrole complexes. synthesis, redox chemistry, photophysical properties and photonic applications", Chem. Soc. Rev. **50** (2021) 12189. https://doi.10.1039/c9cs00828D.

[31] X. Yu, Y. Hu, C. Guo, Z. Chen, H. Wang & X. Li, "Discrete terpyridine-lanthanide molecular and supramolecular complexes, "supramolecular materials **3** (2024) 100074. https://doi.org/10.1016/j.supmat.2022.100017.

[32] C. E. Housecroft & A. G. Sharp, *Inorganic Chemistry*, Third Edition. Pearson Education Limited England, 2018, pp. 722–733. https://books.google.com.ng/books/about/Inorganic_Chemistry.html?id=_1gFM51qpAMC&redir_esc=y.

[33] I. Ali, W. A. Wani & K. Saleem, "Empirical formulae to molecular structures of metal complexes by molar conductance" Synthesis and Reactivity in Inorganic Metal-Organic and NanoMetal Chemistry **43** (2013) 1162. https://doi.org/10.1080/15533174.2012.756898.

[34] A. M. Ajilouni, Z. A. Taha, A. K. Hijazi & W. M. Al-momani, "A series of lanthanide complexes with 2-fluoro-*N'*-(furan-2-ylmethylene) benzohydrazide ligand: Synthesis, characterization, luminescent properties and biological evaluation", Appl. Organomet. Chem. **32** (2018) 2292. https://doi.org/10.1002/aoc.4536.

[35] D. A. Omoboyowa, G. Singh, J. O. Fatoki & O. Oyeneyin, "Computational investigation of phytochemicals from *Abrus precatorius* seeds as modulators of peroxisome proliferator-activated receptor gamma (PPARγ) Journal of biomolecular structure and dynamics **41** (2023) 5568. https://doi.org/10.1080/07391102.2022.2091657.

[36] A. M. May & J. L. Dempsey, "A new era of LMCT: Leveraging ligand-to-metal charge transfer excited state for photochemical reactions", Royal society of chemistry **15** (2024) 6661. https://doi.org/10.1016/j.ica.2023.121697.

[37] J. H. S. Monteiro, "Recent advance in luminescence imaging of biological systems using lanthanide (III) luminescent complexes", molecules **25** (2020) 2089. https://doi.org/10.1016/j.ica.2023.121697.

[38] J. P. Coates, J. Workman & A. W. Sprinsteen, *A Review Of Sampling Methods For Infrared Spectroscopy*, Academic Press, New York, 1998, pp. 49–91. https://doi.org/10.1016/B978-012764070-9%2F50005-6.

[39] W. H. Hegazy & A. Al-Motawa, "Lanthanide Complexes of Substituted β-Diketone Hydrazone Derivatives: Synthesis, Characterization, and Biological Activities", Bioorgaic Chemistry and Application **2011** (2011) 531946. https://doi.org/10.1155/2011/531946.

[40] M. C. Egbujor, U. C. Okoro, S. A. Egu, V. I. Okonkwo, S. N. Okafor, C. N. Emeruwa & D. C. Nwobodo, "Synthesis and biological evaluation of sulfamoyl carboxamide derivatives from sulfur-containing α-Amino acids", Chiang Mai J. Sci. **49** (2022) 1100. https://doi.org/10.12982/CMJS.2022.070.

[41] M. A. Farukh, K. M. Butt, K. Chong & W.S Chang, "Photoluminescence emission behavior on the reduced band gap of Fe doping in CeO₂-SiO₂ nanocomposite and photophysical properties", J. Saudi Chem. Soc. **23** (2019) 561. https://doi.org/10.1016/j.jscs.2018.10.002.

[42] A. B. Kulkarni, S. N. Methad & R. P. Bakale, "The evaluation of kinetic parameters for cadmium doped Co-Zn ferrite using thermogravimetric analysis", Ovidius University Annals of Chemistry **30** (2019) 60. https://doi.org/10.2478/auoc-2019-0011.

[43] M. S. Iorungwa, R. A. Wuana & S. T. Dafa, "Synthesis, Characterization, Kinetics, Thermodynamic and Antimicrobial Studies of Fe(III), Cu(II), Zn(II), N,N'-Bis(2- hydroxy-1,2-

[44] H. I. Ya-Fan, S. Xu , Q. Shi, J. Zhao, N. Ren, J. Gao & J. Zhang, "Novel lanthanide complexes synthesized from 3-Dimethylamino Benzoic acid and 5,5ɩ-Dimethyl-2,2ɩ Bipyridine ligand: crystal structure, thermodynamics, and fluorescence properties", Molecules **28** (2023) 8156. https://doi.org/10.3390/molecules28248156.

[45] Z. A. Piskulich, O. O. Mesele & W. H. Thompson, "Activation energies and beyond", The Journal of Physical Chemistry A **123** (2019) 7185. https://doi.org/10.1021/acs.jpca.9b03967.

[46] P. Jin, Q. Luo, G. K. Gransbury, I. J. Vitorica-Yrezabal, T. Hajdu, I. Strashnow, E. J. Mclnnes, R. E. Winpenny, N. F. Chilton, D. P. Mills & Y. Zheng, "Thermally stable terium (III) and Dysprosium (III) bisamidinate complexes", J. Am. Chem. Soc. **145** (2023) 27993. https://doi.org/10.1021/jacs.3c07978.

[47] E. A. Ivanova , K. S. Smirnova, I. P. Pozdnyakov, A. S. Potapov & E. V. Lider, "Synthesis, crystal structures, and luminescence properties of lanthanide(III) complexes with 1-(1*H*-benzimidazol-1yl-methyl)-1*H*-benzotriazole", Inorganic chimica **557** (2023) 121697. https://doi.org/10.1016/j.ica.2023.121697.

[48] M. Ghhaza, M. Safder, T. Lasttusaari & M. Karppinen, "Amorphous to crystalline transition and photoluminescence switching in guest-absorbing metal organic network thin films", Chem. Commun. **56** (2020) 241. https://doi.org/10.1039/c9cc08904g.

[49] A. M. Ajilouni, Z. A. Taha, A. K. Hijazi & W. M. Al-momani, "A series of lanthanide complexes with 2-fluoro-N'-(furan-2-ylmethylene) benzohydrazide ligand: Synthesis, characterization, luminescent properties and biological evaluation", Appl. Organomet. Chem. **32** (2018) 2292. http://dx.doi.org/10.1002/aoc.4536.

[50] G. A. Thakur, U. N. Dhaigude & P. B. Thakur, "Synthesis, spectral characterization and antibacterial studies of mixed ligand La(III) and Ce(III) complexes derived from 1-nitroso-2-naphthol and some amino acids", Orient Journal Chemistry **36** (2020) 632639. http://dx.doi.org/10.13005/ojc/360406.

[51] . S. B. Vidyasagar, S. Eswaramma & K. Krishna- Rao, "Synthesis, characterization, luminescence and biological activities of lanthanide complexes with a hydrazone ligand", Main group chemistry **17** (2018) 99. http://dx.doi.org/10.3233/MGC-180251.

[52] A. D. Sharma, A. D. Kaur & A. Chauhan, "Molecular docking studies of principal components and *in vitro* inhibitory activities of *Rosmarinus officinalis* essential oil against *Aspergillus flavus, Aspergillus fumigatus* and *Mucor indicus*", Phytomedicine plus **3** (2023) 100493. https://doi.org/10.1016/j.phyplu.2023.100493.

[53] A. Alanio, S. Delli'ere, S. Fodil, S. M. Bretagne & B. M´egarbane, "Prevalence of putative invasive pulmonary aspergillosis in critically ill patients with COVID-19", Lancet. Respir. Med. **8** (202) 48. https://doi.org/10.1016/s2213-2600(20)30237-x.

[54] T. M. John, C. N. Jacob & D. P. Kontoyiannis, " When uncontrolled diabetes mellitus and severe COVID-19 converge: the perfect storm for mucormycosis", J. Fungi **7** (2020) 298. https://doi.org/10.3390/jof7040298.

[55] M. Hoenigl, D. Seidel, R. Sprute, C. Cunha, M. Oliverio, G. H. Goldman, A. S. Ibrahim & A. Carvalho, "COVID-19-associated fungal infections", Nat. Microbiol. **7** (2022) 1127. https://doi.org/10.1038/s41564-022-01172-2.

[56] K. E. Schweer, C. Bangard, K. Hekmat & O. A. Cornely, "Chronic pulmonary aspergillosis", Mycoses **57** (2014) 257. https://doi.org/10.1111/myc.12152.

[57] M. Kumar, G. C. Sahoo, W. A. Ansari, M. A. Ali, M. A. Farah & J. Lee, "Molecular docking analysis of Omt-A protein model from *Aspergillus flavus* with synthetic compounds", J. Bioinformation **19** (2023) 990. https://doi.org/10.6026/97320630019990.

[58] B. K. Kumara, A. R. Lingaiah, P. V. Rao, P. S. Narsaiah, B. Reddy, A. S. K & U.S.N. Murty, "Design, synthesis and biological evaluation of benzimidazole-pyridine- piperidine hybrids as a new class of potent antimicrobial agents", Lett. Drug Des. Discovery **12** (2015) 38. http://dx.doi.org/10.2174/1570180811666140725185713.

[59] M. A. Begam, N. Akalya, N. Murugesan, R. Dass & N. Prakash, "Antimicrobial screening and molecular docking of synthesized 4,6-di(1H-indol-3-yl)-1,6-dihydropyrimidin-2-amine", Intelligent pharmacy **2** (2024) 571577. http://dx.doi.org/10.1016/j.ipha.2024.01.002.

[60] T. Sisay, N. Mainal, S. Wachira & V. A. Mobegi, "In-silico evalua-

tion of fungal and bacterial L-asparaginases allergenicity", Informatics in Medicine Unlocked **43** (2023) 101398. https://doi.org/10.1016/j.imu.2023.101398.

[61] M. Raftani, T. Abram, A. Azaid, R. Kacimi, M./N. Bennani & M. Bouachrine, "Theoretical design of new organic compounds based on diketopyrrolopyrrole and phenyl for organic bulk heterojunction solar cell applications: DFT and TD-DFT study", Materials Today: Proceedings **45** (2021) 7334. https://doi.org/10.1016/j.matpr.2020.12.1228.

[62] M. A. Mumit, T. K. Pal, M. A. M. Alam, M. A. Islam, S. Paul & M. Sheikh, "DFT studies on vibrational and electronic spectra, HOMO–LUMO, MEP, HOMA, NBO and molecular docking analysis of benzyl-3-N-(2,4,5-trimethoxyphenylmethylene)hydrazinecarbodithioate", Journal of molecular structure **1220** (2020) 128715. https://doi.org/10.1016/j.molstruc.2020.128715.

[63] T. Sisay, N. Mainal, S. Wachira & V. A. Mobegi, "In-silico evaluation of fungal and bacterial L-asparaginases allergenicity", Informatics in Medicine Unlocked **43** (2023) 101398. https://doi.org/10.1016/j.imu.2023.101398.

[64] N. Premjanu, C. Jaynthy & S. Diviya, "Antifungal activity of endophytic fungi isolated from lannea coromandelica €" An Insilico Aproach", Int. J. Pharm. Pharm. Sci. **8** (2016) 207. https://journals.innovareacademics.in/index.php/ijpps/article/view/9633.

[65] N. Elangovan, R. Thomas & S. Sowrirajan, "Synthesis of Schiff base (E)-4-((2-hydroxy-3,5-diiodobenzylidene)amino)-N-thiazole-2-yl)benzenesulfonamide with antimicrobial potential, structural features, experimental biological screening and quantum mechanical studies" J. Mol. Struct **1250** (2022) 131762. https://doi.org/10.1016/j.molstruc.2021.131762.

[66] J. Makhlouf, H. Louis, I. Benjamin, E. Ukwenya, A. Valkonen & W. Smirani, "Single crystal investigations, spectral analysis, DFT studies, antioxidants, and molecular docking investigations of novel hexaisothiocyanato chromate complex", J. Mol. Struct **1272** (2023) 134223. https://doi.org/10.1016/j.molstruc.2022.134223.

[67] S. D. Oladipo, A. A. Adeleke, A. A. Badeji, K. I. Babalola, A. H. Labulo, I. Hassan, S. T. Yussuf, S. O. Olalekan, "Computational investigation and biological activity of selected Schiff bases", J. Nig. Soc. Phys. Sci. **6** (2024) 2103. https://doi.org/10.46481/jnsps.2024.2103.

[68] W. Chen, M. Li, W. HiBo, L. Zhiwei, B. Zuqiana & H.Chunhui, "Advances in luminescence lanthanide complexes and applications", Science China technological science **61** (2018) 1. https://doi.org/10.1016/j.ica.2023.121697.

[69] M. C. Egbuhor, U. C. Okoro, S. N. Okafor, P. I. Egwuatu, I. S. Amasiatu & U. B. Amadi, "molecular docking of some Monoazaphenothiazine derivatives as antimicrobial agents", Journal of pharmaceutical research **5** (2020) 60. .